



Dynamic Factor Models for Binary Data in Circular Spaces: An Application to the U.S. Supreme Court

Rayleigh Lei^{1,*} and Abel Rodriguez¹

¹Department of Statistics, University of Washington, 4110 E Stevens Way NE, 98195, Washington, USA

*Corresponding author. rlei13@uw.edu

FOR PUBLISHER ONLY Received on Date Month Year; revised on Date Month Year; accepted on Date Month Year

Abstract

Latent factor models are widely used in the social and behavioral science as scaling tools to map discrete multivariate outcomes into low dimensional, continuous scales. In political science, dynamic versions of classical factor models have been widely used to study the evolution of justice's preferences in multi-judge courts. In this paper, we discuss a new dynamic factor model that relies on a latent circular space that can accommodate voting behaviors in which justices commonly understood to be on opposite ends of the ideological spectrum vote together on a substantial number of otherwise closely-divided opinions. We apply this model to data on nonunanimous decisions made the U.S. Supreme Court between 1937 and 2021, and show that there are at least two periods (1949-1952 and 1967-1970) when voting patterns can be better described by a circular latent space. Furthermore, we show that, for periods for which circular and Euclidean models can explain the data equally well, key summaries such as the ideological rankings of the justices coincide.

Key words: Factor Models, Spatial Voting Model, U.S. Supreme Court, Circular Data, Projected Gaussian Process

1. Introduction

Latent factor models (e.g., see Rummel, 1988 or Cattell, 2012) are a widely-used set of techniques in the social and behavioral sciences. Depending on the context, they are used as either a dimensionality reduction tool to model multivariate data and/or as a scaling tool that maps observed outcomes onto unobserved constructs such as intelligence or ideology. One particularly important example is the class of Item Response Theory (IRT) models (e.g., see Fox, 2010 Embretson and Reise, 2013), in which the observed outcomes are either binary or categorical. These models have been widely used in the applications in psychometry (e.g., Reise and Rodriguez, 2016 and Paganin et al., 2022) and clinical assessment (e.g., Thomas, 2011), among other disciplines. In the context of political science applications, IRT models can be derived as special cases of the celebrated class of spatial voting models (Davis et al., 1970; Enelow and Hinich, 1984; Poole and Rosenthal, 1985; Jackman, 2001).

An important extension of latent factor models considers situations where the observed data consists of multivariate time series and the latent factors are allowed to evolve over time (e.g., see Barhoumi et al., 2013 and Stock and Watson, 2016). Versions of these models that allow for categorical observations were originally developed in Forni et al. (2000) and Peña and Poncela (2004), and have seen applications in a wide range of disciplines (e.g., see Bellégo and Ferrara, 2012, Fountas et al., 2018 and Angelopoulos et al., 2020). In this paper, we are interested in the application of such models to the estimation of preferences in deliberative bodies such as legislatures and multi-judge courts.

In political science, Martin and Quinn (2002) pioneered the use of dynamic factor models by extending the work of Jackman (2001) to study the evolution of preferences of justices in the U.S. Supreme Court. Their highly-cited paper has been extremely impactful, both because of the innovative nature of the methodology, and because of the substantive contribution to the understanding of the behavior of U.S. Supreme Court justices. Indeed, estimates of justices' preferences are the foundation upon which accounts of policy-motivated behavior of Supreme Court justices are built, and the topic has received attention in the political science and legal studies literatures since at least the mid 60s (e.g., see Schubert, 1965, Rohde and Spaeth, 1976, Segal and Cover, 1989 and Epstein et al., 2007). Accordingly, the Martin-Quinn scores have been widely used as inputs for further analyses of justices behavior (e.g., see Black and Owens, 2009, Casillas et al., 2011 and Owens and Wedeking, 2011). Furthermore, the underlying methodology has been applied in other areas of political science (e.g., see Bailey et al., 2017, Bertomeu et al., 2017, and Lo, 2018) and extended by various authors (e.g., see Bailey, 2007, Linzer and Staton, 2015 and Kovac et al., 2019).

Most widely-used spatial voting models (including Poole and Rosenthal, 1985, Jackman, 2001 and Martin and Quinn, 2002) assume that voters' preferences (their *ideal points*) lie in a low-dimensional Euclidean space. However, while the choice of a Euclidean geometry makes intuitive sense and allows for a straightforward interpretation of the model, it can fail to properly describe situations in which extreme actors prefer similar outcomes, but for different ideological reasons. As an alternative, circular geometries for the latent space have been proposed, with early examples including Weisberg (1974) and Mokken et al. (2001). Recently, Yu and Rodríguez (2021) proposed a Bayesian factor model for binary data that uses a circular policy space and applied it to the study of voting behavior in the U.S. House of Representatives. Their results indicate that, starting with the 112th House (which met between January 3, 2011, and January 3, 2013), the behavior of the chamber has been better explained by a circular geometry.

Accounting for the geometry of the latent policy space is particularly important when modeling the voting behavior of the U.S. Supreme Court, where justices at opposite ends of the ideological spectrum often vote in similar ways, albeit for very different reasons. For instance, despite Justice Neil Gorsuch's reputation as an originalist and the fact that he voted with Justice Clarence Thomas over 60% of the time in nonunanimous cases during the 2019 term, he also voted with Justices Sonya Sotomayor and Ruth Bader Ginsburg about 40% of the time in these types of cases (Harvard Law Review, 2022). Furthermore, while the majority of five-four decisions from 2012-2020 were decided by the five conservative justices, there are numerous instances of very conservative justices, such as Justices Antonin Scalia and Thomas, voting with very liberal justices, such as Justices Sotomayor and Ginsburg. More generally, the use of circular voting spaces can provide a natural explanation to historical conundrums such as that presented by the voting behavior of justice Felix Frankfurter (please see Section 5). While Frankfurter is often seen as becoming more and more conservative despite his liberal activism before joining the court (e.g., see Lepore, 2014), this reputation is at odds with the ranking provided by the Martin-Quinn scores, which place him as the median justice in the 1953 term.

In this paper, we extend the framework of Yu and Rodríguez (2021) to construct a Bayesian dynamic factor model with a circular latent space, and apply it to the study of the evolution of U.S. Supreme Court justices' revealed preferences since 1937. Our proposal uses a generalization of the projected Gaussian distributions (Mardia et al., 2000; Small, 2012) to model the distribution of the justices' ideal points. More specifically, the evolution of the ideal points for each justice is modeled using a (stationary) matrix-variate first-order autoregressive processes as the joint distribution for a set of latent Gaussian distributions, which are then used to induce an autoregressive prior distribution on circular coordinates. The resulting model for the ideal points can be seen as a special case of the projected Gaussian process introduced in Wang and Gelfand (2014), leading to straightforward computational algorithms based on elliptical slice samplers (Murray et al., 2010).

An alternative approach to model voting records in which "extremes" vote together is the unfolding model recently introduced by Duck-Mayr and Montgomery (2022), which is in turn based on the work of Roberts et al. (2000). This model is, however, designed for static settings in which ideal points are constant, and is not appropriate for studying the evolution of justices ideal points over time. We are not aware of any extensions of this model to dynamic settings, which are not straightforward because of the associated computational challenges. Another alternative for handling extremes voting together was presented in Spirling and Quinn (2010), who developed a clustering algorithm based on Dirichlet process mixtures to identify voting blocks within a deliberative body. Their approach was later extended to dynamic settings by Crane (2017), who used it to study the U.S. Supreme Court. The voting blocks identified by these methods can provide interesting insights on their own.

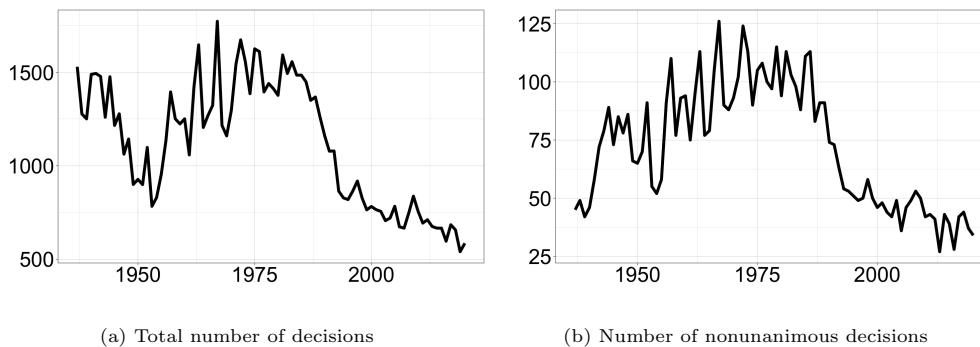


Fig. 1: Number of decisions made by the U.S. Supreme Court on each term between 1937 and 2021.

However, they do not yield the kind of scaling of justices preferences in a continuous scale that is most useful in downstream applications.

The remainder of the paper is organized in the following manner. Section 2 provides some background information about the U.S. Supreme Court data that motivates our approach. Section 3 introduces our dynamic circular voting model and explores some of its properties. Section 4 reviews our computational strategy, which relies on Markov chain Monte Carlo algorithms to generate approximate samples of the associated posterior distribution. Section 5 presents the results of our analysis of the U.S. Supreme Court voting data. Finally Section 6 discusses some of the limitations of the model as well as further extensions.

2. Motivating data set: voting patterns in the U.S. Supreme Court

The U.S. Supreme Court (SCOTUS) is the highest court in the federal judiciary of the United States, having ultimate appellate jurisdiction over all U.S. federal court cases and over state court cases that involve a point of U.S. constitutional or federal law. Since 1869, SCOTUS has been composed of nine justices. In principle, all sitting judges participate in every case taken on by the court, and decisions are made by a majority vote of all the participating judges.

For this paper, we use the 1937-2021 data set available at <https://mqscores.lsa.umich.edu/>. As in Martin and Quinn (2002), we work with nonunanimous decisions that are either formally decided cases with written opinions after full oral arguments, or cases decided by an equally divided vote. The outcome of the justices' votes are encoded so that a justice's vote is set to 1 if the vote supported a reversal of a lower court's decision, and 0 otherwise. Note that most SCOTUS decisions end up reversing lower court ones (only 98 were affirmed in this particular data set, 1.61% of nonunanimous decisions). Equally divided votes might happen if seats are vacant or if a justice recuses themselves (a rare situation), in which case the lower Court stands but no precedent is set. Figure 1 shows both the total number of decisions and the number of nonunanimous decisions during each term between 1937 and 2020. These graphs show that the number of decisions made each term varies considerably. In particular, the total number of cases decided by SCOTUS started to decline in the early 1980s, with the number of nonunanimous decisions following a similar pattern. While, in general, the number of nonunanimous decisions represents a relatively small percentage of the total number of decisions issued by the court, the percentage is particularly low at the very beginning of the time series. This phenomenon was likely driven by a strong belief among the justices that the legitimacy of the court at the time heavily depended on its unanimity (Feldman, 2010).

There were a total of 48 Supreme Court justices between 1937 and 2020, serving anywhere between one and 38 full or partial terms (see Figure 2a). Virtually all these justices served their terms in consecutive years. The only exception is Justice Robert Jackson, who took a leave of absence during the 1945 term to serve as Chief United States Prosecutor during the Nuremberg trials. With the exception of four justices who either retired or died in the 1937 or 1938 terms, justices on average voted in 97.5% of the cases taken up by the court during their terms (see Figures 2b and 2c).

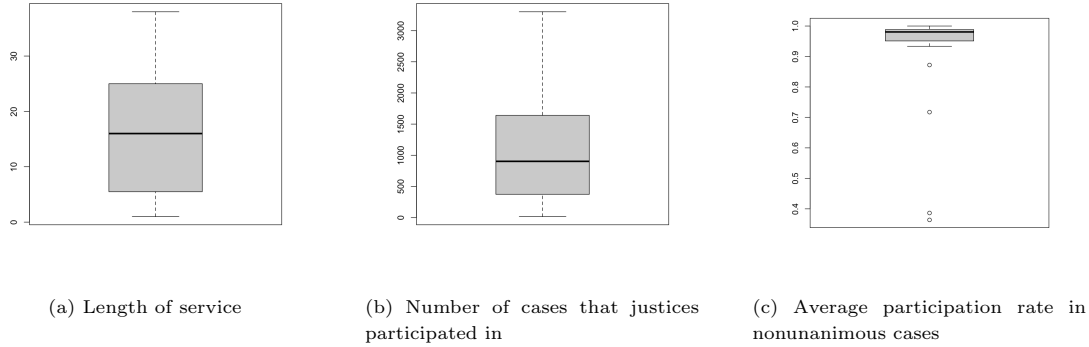


Fig. 2: Length of service and participation rates for Supreme Court justices between 1937 and 2021.

3. Model formulation

Let $y_{i,j,t}$ denote the vote of justice i on the j -th decision taken in term t , where $i = 1, \dots, I$, $t = 1, \dots, T$, and $j = 1, \dots, J_t$. As discussed in the previous section, we set $y_{i,j,t} = 1$ if the vote was to affirm the lower court decision, and $y_{i,j,t} = 0$ otherwise. Because there are only up to 9 justices in the Supreme Court at any given time, a large number of the $y_{i,j,t}$ are unobserved. It is quite reasonable to treat these missing values as missing completely at random (MCAR) (Enders, 2010; Rodriguez and Moser, 2015). We make the same assumption about the values of $y_{i,j,t}$ that are missing because of any other reasons, such as recusals. While the MCAR assumption is somewhat harder to justify in the case of recusals, it is common in the literature. Furthermore, as we discussed in the previous section, the number of recusals in our data set is very low (recall Figure 2c) and we expect that, even if the MCAR assumption is incorrect, its impact will be minimal.

We construct our model using the random utility framework introduced in McFadden (1973). We assume that each justice has two utility functions U_A and U_R , one associated with voting to affirm the lower court decision, and one associated with reversing it. These functions depend on the ideal point of the justice during term t , $\beta_{i,t}$, which lives in a latent space \mathcal{S} , and of two decision-specific positions ($\psi_{j,t}$ and $\zeta_{j,t}$, also in \mathcal{S}) that represent votes to affirm or reverse the j -th lower court decision during term t :

$$U_A(\psi_{j,t}, \beta_{i,t}) = -d^2(\psi_{j,t}, \beta_{i,t}) + \nu_{i,j,t}, \quad U_R(\zeta_{j,t}, \beta_{i,t}) = -d^2(\zeta_{j,t}, \beta_{i,t}) + \epsilon_{i,j,t},$$

where $d(\cdot, \cdot)$ is an appropriate distance function defined on \mathcal{S} , and $\nu_{i,j,t}$ and $\epsilon_{i,j,t}$ are mutually independent random shocks such that $\nu_{i,j,t} - \epsilon_{i,j,t}$ is distributed with density $g_{\kappa_{j,t}}$. An affirmative vote occurs if and only if $U_A(\psi_{j,t}, \beta_{i,t}) > U_R(\zeta_{j,t}, \beta_{i,t})$, i.e.,

$$\begin{aligned} \Pr(y_{i,j,t} = 1 \mid \beta_{i,t}, \psi_{j,t}, \zeta_{j,t}) &= \Pr(U_A(\psi_{j,t}, \beta_{i,t}) > U_R(\zeta_{j,t}, \beta_{i,t})) \\ &= \Pr(\nu_{i,j,t} - \epsilon_{i,j,t} > d^2(\psi_{j,t}, \beta_{i,t}) - d^2(\zeta_{j,t}, \beta_{i,t})) \\ &= G_{\kappa_{j,t}}(d^2(\zeta_{j,t}, \beta_{i,t}) - d^2(\psi_{j,t}, \beta_{i,t})), \end{aligned}$$

where $G_{\kappa_{j,t}}$ is the cumulative distribution function associated with $g_{\kappa_{j,t}}$. In other words, the model assumes that justice i is more likely to affirm decision j at time t if $\beta_{i,t}$ is closer to $\psi_{j,t}$ than to $\zeta_{j,t}$, with the uncertainty coming from the random $\nu_{i,j,t}$ and $\epsilon_{i,j,t}$.

The model introduced by Martin and Quinn (2002) assumes that $\beta_{i,t}, \psi_{j,t}, \zeta_{j,t} \in \mathbb{R}$, $d(x_1, x_2) = d_E(x_1, x_2) = |x_1 - x_2|$ is the Euclidean distance between the two points, and $\nu_{i,j,t} - \epsilon_{i,j,t}$ follows a standard normal distribution for all j and t . Instead, in this paper we assume that \mathcal{S} corresponds to the unit-radius circle and the coordinates $\beta_{i,t}, \psi_{j,t}, \zeta_{j,t} \in [-\pi, \pi)$ are given in terms of angles (i.e., the polar representation of the points) with respect to a reference (which we select as the upper pole of the circle, please see Figure 3). The most appropriate distance metric in this context is the geodesic distance on the unit circle, $d(x_1, x_2) = d_G(x_1, x_2) = \arccos(\cos(x_1 - x_2))$,

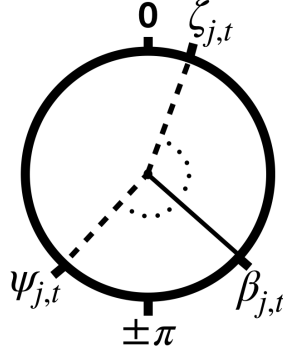


Fig. 3: A circular policy space.

the smallest angle between x_1 and x_2 . This formulation implies that

$$\Pr(y_{i,j,t} = 1 \mid \beta_{i,t}, \psi_{j,t}, \zeta_{j,t}) = G_{\kappa_{j,t}}(\{\arccos(\cos(\zeta_{j,t} - \beta_{i,t}))\}^2 - \{\arccos(\cos(\psi_{j,t} - \beta_{i,t}))\}^2). \quad (1)$$

Unlike the Euclidean distance, the geodesic distance on the circle takes values on $[0, \pi]$. This implies that $e_{i,j,t} = d_G^2(\zeta_{j,t}, \beta_{i,t}) - d_G^2(\psi_{j,t}, \beta_{i,t}) \in [-\pi^2, \pi^2]$ for any $\psi_{j,t}$, $\zeta_{j,t}$ and $\beta_{i,t}$. To account for this, we assume that $\nu_{i,j,t} - \epsilon_{i,j,t}$ follows a shifted and scaled symmetric beta distribution with density

$$g_{\kappa_{j,t}}(z) = \frac{\Gamma(2\kappa_j)}{2\pi^2 \Gamma(\kappa_j) \Gamma(\kappa_j)} \left(\frac{\pi^2 + z}{2\pi^2}\right)^{\kappa_j - 1} \left(\frac{\pi^2 - z}{2\pi^2}\right)^{\kappa_j - 1}, \quad z \in [-\pi^2, \pi^2], \quad (2)$$

and cumulative distribution function $G_{\kappa_{j,t}}(z) = \int_{-\pi^2}^z g_{\kappa_{j,t}}(u) du$.

Yu and Rodríguez (2021) discuss some of the advantages associated with this formulation. One of its key features is that it can provide a very good approximation to the Euclidean model with a probit link when the data supports this simpler model, while providing additional flexibility when the data does not. Indeed, as the positions $\beta_{i,t}$, $\psi_{j,t}$, $\zeta_{j,t}$ tend to concentrate around an arbitrary common location (say, the upper pole of the circle) the geodesic distance between them becomes approximately equal to their Euclidean distance. Similarly, the distribution in (2) converges in distribution to a Gaussian as $\kappa_j \rightarrow \infty$. On the other hand, when the latent coordinates are spread over the circle, the model can accommodate voting patterns in which justices that are typically understood as being opposite extremes in terms of their preferences vote together (see Figures 4a and 4b for examples that arise in our analysis of the SCOTUS data). This is a behavior that cannot be accommodated by traditional Euclidean voting models. One consequence of this lack of fit is that Euclidean models tend to downweight or outright discard the information provided by these votes. An illustration of this phenomenon can be seen in Figures 4c and 4d, which show equivalent results under the Euclidean model of Martin and Quinn (2002) for the same two decisions. Indeed, note that the affirm and reverse positions in Figure 4d are very close to each other, which implies that justices' preferences do not explain the results of this vote. While this makes sense under the assumptions of the Euclidean model, it clearly demonstrates that information is not being effectively used. In fact, when “circular” votes are common, the Euclidean model can make extreme justices who participate in them look like centrists, as that is the only explanation for their behavior that is allowed by the model.

3.1. A hierarchical model for the evolution of revealed preferences on the circle

One of the key goals of our model is to understand how the preferences of justices have changed over time. To do this, we propose to use a joint prior for the vector of ideal points of a given judge, $\beta_i = (\beta_{i,1}, \dots, \beta_{i,T})'$, while additionally assuming independence across justices. To construct such prior, we introduce two independent auxiliary vectors of real-valued random variables $\mathbf{v}_i = (v_{i,1}, \dots, v_{i,T})'$ and $\mathbf{w}_i = (w_{i,1}, \dots, w_{i,T})'$ that follow stationary first-order autoregressive processes with common autocorrelation parameters but potentially different

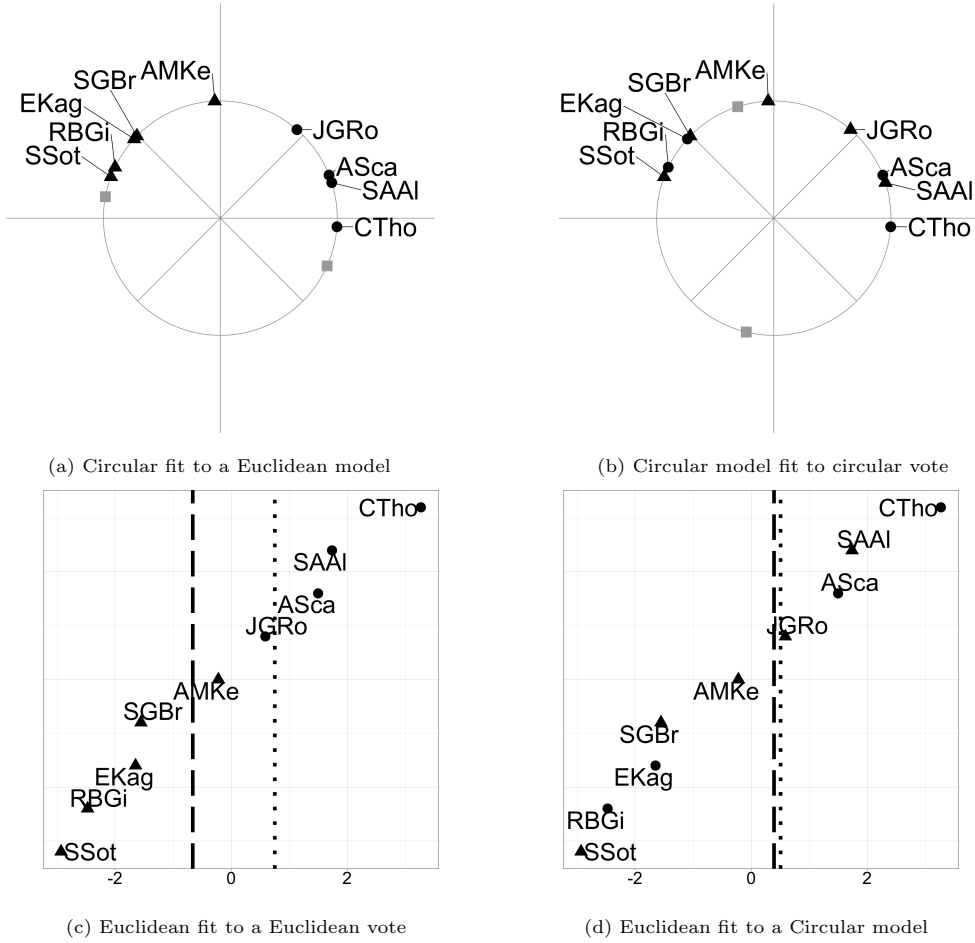


Fig. 4: Examples of Euclidean (left column) and circular (right column) 5-4 votes in the U.S. Supreme Court during the 2014 term. The top row provides the estimates of the model parameters under our circular model, while the bottom row provides the estimates under the (Martin and Quinn, 2002) model for the same two votes. Triangles indicate justices who voted to reverse a lower court decision whereas circles indicate justices who voted to affirm a lower court decision. In the top row, the positions of voting to affirm and reject the decisions are shown with grey squares. In the bottom row, these positions are shown as a dotted and a dashed line, respectively.

means and evolution variances,

$$v_{i,t} | v_{i,t-1} \sim \mathcal{N}(v_{i,t} | \mu_1 + \rho(v_{i,t-1} - \mu_1), \tau_1^2), \quad v_{i,1} \sim \mathcal{N}\left(\mu_1, \frac{\tau_1^2}{1 - \rho^2}\right), \quad (3)$$

$$w_{i,t} | w_{i,t-1} \sim \mathcal{N}(w_{i,t} | \mu_2 + \rho(w_{i,t-1} - \mu_2), \tau_2^2), \quad w_{i,1} \sim \mathcal{N}\left(\mu_2, \frac{\tau_2^2}{1 - \rho^2}\right), \quad (4)$$

where $\mathcal{N}(x | a, b)$ denotes the Gaussian distribution with mean a and variance b , and $\rho \in [-1, 1]$. Then, the distribution for $\beta_i = (\beta_{i,1}, \dots, \beta_{i,T})$ is obtained through a transformation of v_i and w_i such that

$$\beta_{i,t} = \text{atan2}(v_{i,t}, w_{i,t}) = \begin{cases} \arctan\left(\frac{w_{i,t}}{v_{i,t}}\right) & v_{i,t} \geq 0, \\ \arctan\left(\frac{w_{i,t}}{v_{i,t}}\right) + \pi & v_{i,t} < 0, w_{i,t} \geq 0, \\ \arctan\left(\frac{w_{i,t}}{v_{i,t}}\right) - \pi & v_{i,t} < 0, w_{i,t} < 0. \end{cases} \quad (5)$$

The joint density of β_i is then

$$p(\beta_i | \rho, \mu_1, \mu_2, \tau_1, \tau_2) = \frac{1}{2\pi\tau_1\tau_2} |\Omega(\rho)|^{1/2} \int_0^\infty r \exp \left\{ -\frac{1}{2} \text{tr} U^T(r, \beta_i, \mu_1, \mu_2, \tau_1, \tau_2) \Omega(\rho) U(r, \beta_i, \mu_1, \mu_2, \tau_1, \tau_2) \right\} dr, \quad (6)$$

where $\Omega(\rho)$ is a $T \times T$ tridiagonal matrix and $U(\beta, \mu_1, \mu_2, \tau_1, \tau_2)$ is a $T \times 2$ matrix:

$$\Omega(\rho) = \begin{pmatrix} 1 & -\rho & 0 & \cdots & 0 & 0 \\ -\rho & 1 + \rho^2 & -\rho & \cdots & 0 & 0 \\ 0 & -\rho & 1 + \rho^2 & \cdots & 0 & 0 \\ \vdots & \vdots & \vdots & \ddots & \vdots & \vdots \\ 0 & 0 & 0 & \cdots & -\rho & 1 \end{pmatrix}, \quad U(r, \beta, \mu_1, \mu_2, \tau_1, \tau_2) = \begin{pmatrix} \frac{r \cos \beta_1 - \mu_1}{\tau_1} & \frac{r \sin \beta_1 - \mu_2}{\tau_2} \\ \frac{r \cos \beta_2 - \mu_1}{\tau_1} & \frac{r \sin \beta_2 - \mu_2}{\tau_2} \\ \vdots & \vdots \\ \frac{r \cos \beta_T - \mu_1}{\tau_1} & \frac{r \sin \beta_T - \mu_2}{\tau_2} \end{pmatrix}. \quad (7)$$

This distribution defines an autoregressive process on the circle with stationary distribution given by a projected Gaussian distribution (Mardia et al., 2000; Small, 2012):

$$p_0(\beta) = \frac{1 - \rho^2}{2\pi\tau_1\tau_2} \int_0^\infty r \exp \left\{ -\frac{1 - \rho^2}{2} \left[\left(\frac{r \cos \beta - \mu_1}{\tau_1} \right)^2 + \left(\frac{r \sin \beta - \mu_2}{\tau_2} \right)^2 \right] \right\} dr.$$

The prior in (6) is a special case of the projected Gaussian process introduced in Wang and Gelfand (2014) with an exponential covariance function evaluated on a uniform grid over time. The value of ρ controls the level of temporal dependence (with $\rho = 0$ leading to independent priors on the ideal point of each judge during each term), the ratio μ_1/μ_2 determines the mean value of the stationary distribution, and the value of $\mu_1^2 + \mu_2^2$ together with $\tau_1^2/(1 - \rho^2)$ and $\tau_2^2/(1 - \rho^2)$ control the variance of the stationary distribution, as well as its kurtuosis and whether it is a unimodal or bimodal distribution. We further discuss the interpretation of the parameters in Section 3.2 below and in Section 1 of the supplementary materials.

To complete the model, we need to elicit priors on the ‘‘affirm’’ and ‘‘reversing’’ positions $\psi_{j,t}$ and $\zeta_{j,t}$, as well as the scaling parameters $\kappa_{j,t}$ controlling the precision (inverse variance) of the link function. In particular, $\psi_{j,t}$ and $\zeta_{j,t}$ are assumed to be independent from each other and across all decisions. Furthermore, in order to enable the model to accommodate the full spectrum of potential voting patterns, we assign each of these parameters a uniform distribution on the circle (recall Figure 4). On the other hand, we assume that the precision parameters for the link function are independently distributed from an exponential distribution with mean λ . The value of λ is assumed unknown and assigned an appropriate hyperprior (see next Section).

3.2. Hyperprior elicitation

In this section we discuss the main considerations associated with the selection of the hyperpriors for our model, and how these drive our selection in the context of the U.S. Supreme Court data discussed in Section 2. Alternative values for the hyperparameters are discussed as part of our sensitivity analysis in Section 5.3.

We consider first the hyperpriors on the parameters μ_1 , μ_2 , τ_1 , τ_2 and ρ for the projected autoregressive process. In order to ensure that the ideal points are (weakly) identifiable, we need to fix the prior mean of the stationary distribution of the process. We achieve this by setting $\mu_2 = 0$, which implies that the expected value of $\beta_{i,t}$ is zero. A second consideration has to do with our assumptions about the evolution of justice’s preferences, which we expect, for the most part, to drift only slowly over time. Based on this, we prefer priors that put high probability on values of ρ that are close to 1. More specifically, in our analyses we assigned ρ a Gaussian distribution with mean 0.9 and standard deviation 0.04, truncated to the $[0, 1]$ interval. This prior implies that, a priori, $\Pr(0.85 \leq \rho \leq 1) \approx 0.9$. Then, the priors on $\mu_1 = \mu$, $\tau_1^2 = \tau^2$ and $\tau_2^2 = \zeta\tau^2$ are selected so that the implied stationary distribution on $\beta_{i,t}$ is unimodal and places the majority of its mass on the $[-\pi/2, \pi/2]$ interval. This choice reflects our prior belief that the Euclidean voting model is a good starting point for inference. In the analyses we present in Section 5, μ follows a normal distribution with mean 0 and standard deviation 1.4, truncated to the positive numbers, τ^2 follows an exponential distribution with mean 0.1, and ζ follows a Gamma distribution with mean 1 and variance 0.5. A histogram created from 10,000 samples of the prior on $\beta_{i,t}$ implied by this specific choice of hyperpriors can be seen in Figure 5a.

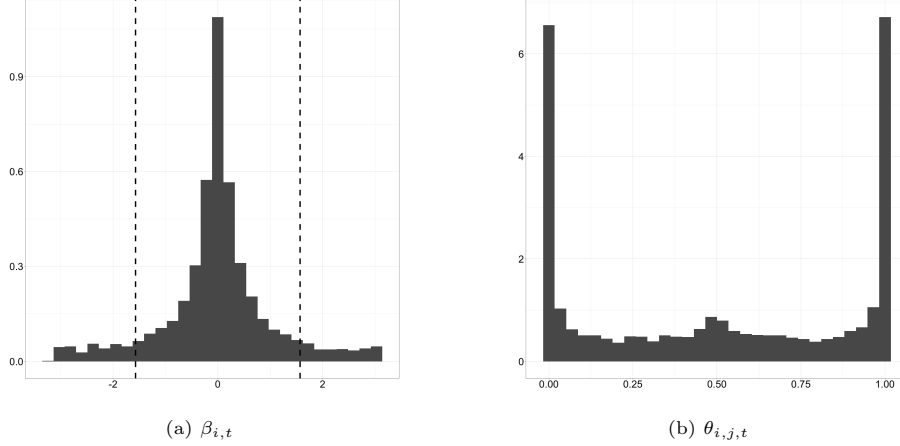


Fig. 5: Histograms showing 10,000 draws from the marginal prior distribution for $\beta_{i,t}$ and $\theta_{i,j,t}$. The left plot is for $\beta_{i,t}$ whereas the right plot is for $\theta_{i,j,t}$. Dashed black lines show the location of $-\frac{\pi}{2}$ and $\frac{\pi}{2}$ for $\beta_{i,t}$.

To specify the prior distribution on λ (the common mean of the precision parameters associated with the link function) we focus on the implied prior on

$$\theta_{i,j,t} = G_{\kappa_{j,t}} \left(\left\{ \arccos(\cos(\zeta_{j,t} - \beta_{i,t})) \right\}^2 - \left\{ \arccos(\cos(\psi_{j,t}, \beta_{i,t})) \right\}^2 \right), \quad (8)$$

the probability that a justice votes to affirm a lower court decision. Note that, under our hyperpriors, this implied prior is the same for every i, j and t . As noted in Spirling and Quinn (2010), we typically want the prior on this parameter to favor values that are close to either 0 or 1. With this in mind, we set the hyperprior for $1/\lambda$ to be an exponential distribution with mean 25. The implied prior on $\theta_{i,j,t}$ can be seen in Figure 5b.

4. Computation

The posterior distribution associated with our model is analytically intractable. Therefore, we rely on a Markov chain Monte Carlo algorithm to generate realizations from the posterior distribution. This is accomplished by iteratively sampling from the full conditional distribution of (blocks of) parameters. Posterior summaries of interest can then be approximated using their empirical counterparts.

To jointly sample from the posterior distribution of each of the ideal point sequence β_i , we employ an elliptical slice sampler (Murray et al., 2010) that relies on the auxiliary variables v_i and w_i defined in (3) and (4). Generally speaking, the elliptical slice sampler was developed to draw samples for random variables whose density can be decomposed as the product of the kernel of a zero-mean Gaussian kernel and an arbitrary function. In our case, conditioning on the remaining parameters, we work with the reparameterization

$$\mathbf{Z}_i = \begin{pmatrix} z_{i,1,1} & z_{i,1,2} \\ z_{i,2,1} & z_{i,2,2} \\ \vdots & \vdots \\ z_{i,T,1} & z_{i,T,2} \end{pmatrix} = \begin{pmatrix} v_{i,1} - \mu & w_{i,1} \\ v_{i,2} - \mu & w_{i,2} \\ \vdots & \vdots \\ v_{i,T_i} - \mu & w_{i,T_i} \end{pmatrix},$$

and focus on sampling \mathbf{Z}_i from its full conditional distribution

$$p(\mathbf{Z}_i | \dots) \propto \exp \left\{ -\frac{1}{2\tau^2} \text{tr} [\boldsymbol{\Sigma} \mathbf{Z}_i^T \boldsymbol{\Omega}(\rho) \mathbf{Z}_i] \right\} \prod_{t=1}^T \prod_{j=1}^{J_t} \{ \theta(z_{i,t,1}, z_{i,t,2}) \}^{y_{i,j}} \{ 1 - \theta(z_{i,t,1}, z_{i,t,2}) \}^{1-y_{i,j}},$$

where $\boldsymbol{\Sigma} = \text{diag}\{1, 1/\varsigma\}$, $\boldsymbol{\Omega}(\rho)$ was defined in (7), and

$$\theta(z_{i,t,1}, z_{i,t,2}) = G_{\kappa_{j,t}} \left(\left\{ d^*(\zeta_{j,t}, z_{i,t,1} + \mu, z_{i,t,2}) \right\}^2 - \left\{ d^*(\psi_{j,t}, z_{i,t,1} + \mu, z_{i,t,2}) \right\}^2 \right),$$

with $d^*(\xi, z_1, z_2) = \arccos(\cos(\xi - \text{atan2}(z_1, z_2)))$. The elliptical slice sampler proceeds by first drawing an auxiliary matrix U^* from a matrix normal distribution,

$$U^* \mid \tau^2, \varsigma, \rho \sim \text{MN}(U^* \mid \mathbf{0}, \Omega^{-1}(\rho), \tau^2 \Sigma^{-1}),$$

along with a random threshold $c \sim \text{Unif}[0, 1]$ and a random angle $a \sim \text{Unif}[0, 2\pi)$. A proposal is then generated as $Z_i^* = \cos(a)Z_i + \sin(a)U^*$, and this proposal is accepted if the ratio

$$\frac{\prod_{t=1}^T \prod_{j=1}^{J_t} \left\{ \theta(z_{i,t,1}^*, z_{i,t,2}^*) \right\}^{y_{i,j}} \left\{ 1 - \theta(z_{i,t,1}^*, z_{i,t,2}^*) \right\}^{y_{i,j}}}{\prod_{t=1}^T \prod_{j=1}^{J_t} \left\{ \theta(z_{i,t,1}, z_{i,t,2}) \right\}^{y_{i,j}} \left\{ 1 - \theta(z_{i,t,1}, z_{i,t,2}) \right\}^{y_{i,j}}}$$

is greater than c . If the proposal Z_i^* is rejected, a new value of a is sampled from a uniform distribution with a curtailed support and the corresponding Z_i^* is either accepted or rejected. This process is repeated until either the proposal is accepted or the support for a becomes empty. Note that the auxiliary matrix U^* and the threshold c remain the same for every proposed Z_i^* within a given iteration of the algorithm.

For the hyperparameters associated with the projected autoregressive process, note that the full conditional posterior distribution for ρ given the random vectors v_i and w_i reduces to a distribution that is almost proportional to a truncated Gaussian distribution. Hence, for this parameter, we develop a Metropolis-Hastings algorithm with independent proposals that has very high acceptance probabilities. On the other hand, while we can directly sample from the individual full conditionals of μ , τ and ς , the very high autocorrelation among these three parameters leads us to prefer a trivariate random walk Metropolis Hastings algorithm to sample from their joint full conditional posterior distribution. The variance-covariance matrix of the proposal distribution is tuned to target an approximate 30% acceptance rate.

The parameters associated with voting to affirm or reverse a given decision, $(\zeta_{j,t}, \psi_{j,t})$, are sampled jointly using a Hamiltonian Monte Carlo algorithm that uses independent von Mises distributions for their momentum. The algorithm is tuned to target an approximate 65% acceptance rate. Next, each $\kappa_{j,t}$ is sampled using univariate random walk Metropolis-Hastings algorithms with proposal distributions tuned to target a 40% average acceptance rate on average. Finally, λ is sampled via a Gibbs sampler because of conjugacy. Full details of the MCMC strategy can be seen in Section 2 of the online supplementary materials and in the implementation available at https://github.com/rayleigh/circ_supreme_court.

4.1. Parameter identifiability

The likelihood function in (1) is invariant to shifts, reflections and wrapping of the latent space. This means that model parameters are not identifiable from the likelihood alone. We already mentioned in Section 3.2 that we address invariance to shifts in the latent space by centering the prior of the ideal points at zero, leading to weak identifiability in the posterior distribution. On the other hand, we address the invariance to wrappings and reflections by postprocessing the samples generated by the MCMC algorithm. In particular, invariance to wrapping is addressed by mapping all angles to the $[-\pi, \pi]$ interval, and invariance to reflexions by fixing the sign of the ideal point of a selected number of justices. In the case of the application to the U.S. Supreme Court discussed in Section 5, this involves making the ideal points of Justice William Douglas negative every term between 1938 to 1966, that of Justice Thurgood Marshall also negative from 1967 to 1990, and that of Justice Clarence Thomas positive from 1991 on.

It is important to note here that, unlike models with Euclidean latent spaces, models based on circular spaces do not suffer from invariance to rescalings of the latent space. This follows from the fact that distances in the latent circular space are bounded from above by π . One consequence of this is that the concentration parameters $\kappa_{j,t}$ s are identifiable from the data without the need to introduce additional constraints.

4.2. Ideological rankings based on circular models

One challenge associated with interpreting the results from our circular model is that the circle is not endowed with a natural total ordering. In order to generate (approximate) rankings under our model, we “unfold” the circle onto the interval $[-\pi, \pi]$ and rank justices on the implied linear scale. As discussed in Yu and Rodríguez (2021), this process has a strong justification when the all the ideal points can be mapped within a semicircle. In other circumstances, these ranks need to be interpreted carefully (please see Section 5.1).

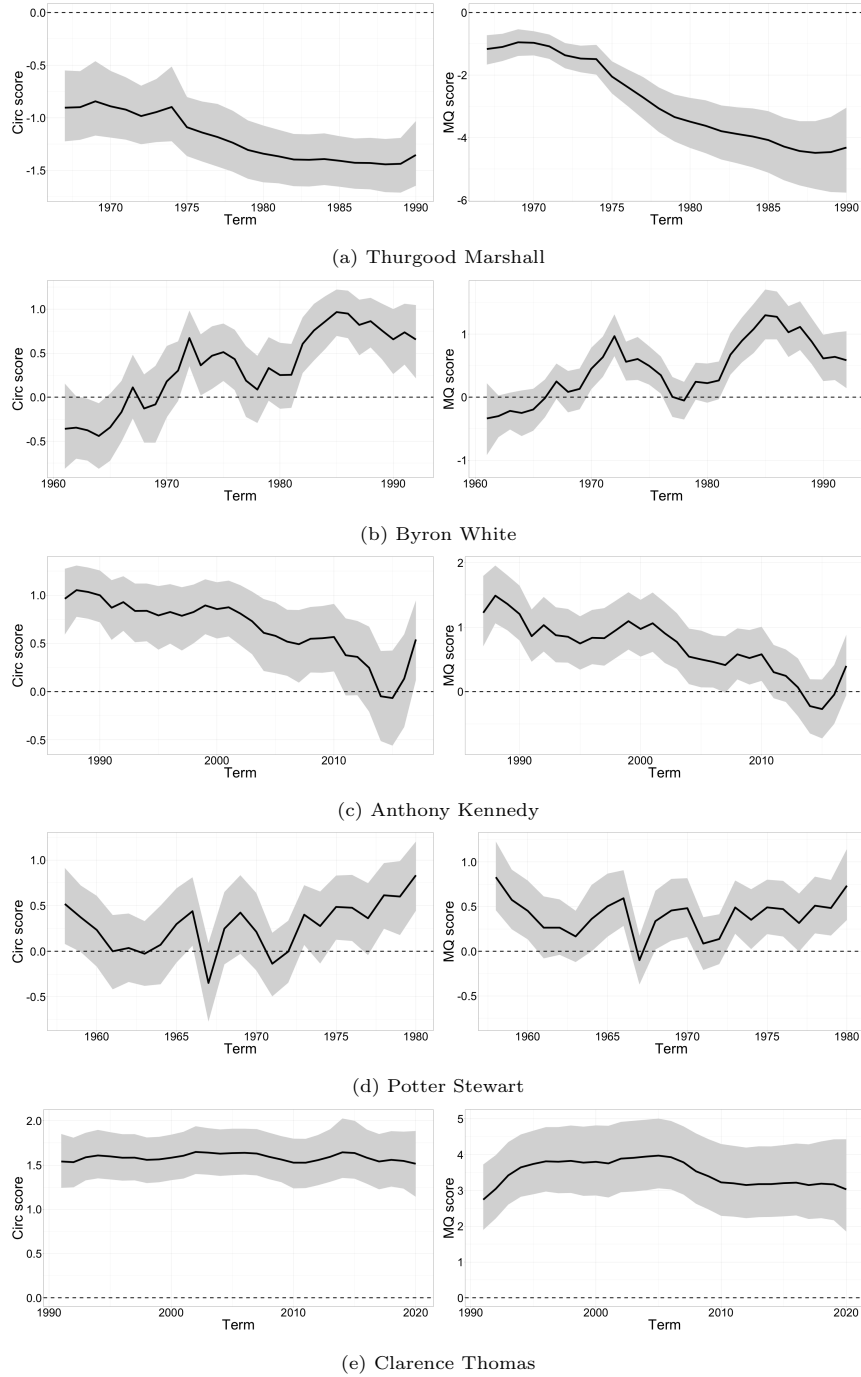


Fig. 6: Posterior mean (solid line) and 95% credible intervals for the ideal points of justices Thurgood Marshall, Byron White, Anthony Kennedy, Potter Stewart, and Clarence Thomas. The left column displays estimates based on our circular model, whereas the right column displays the MQ scores.

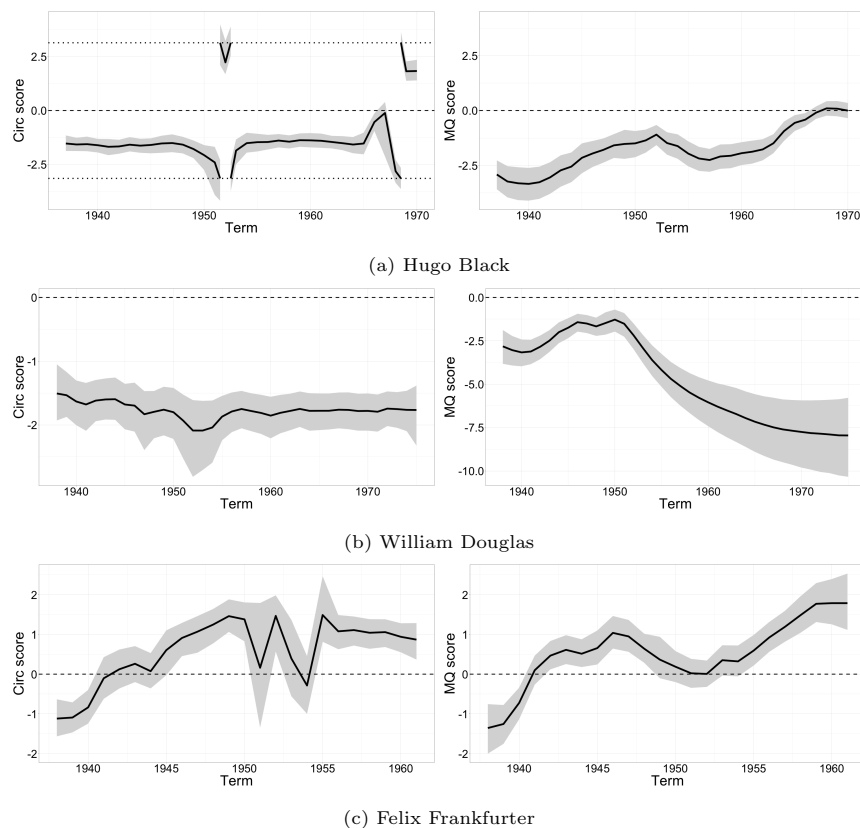
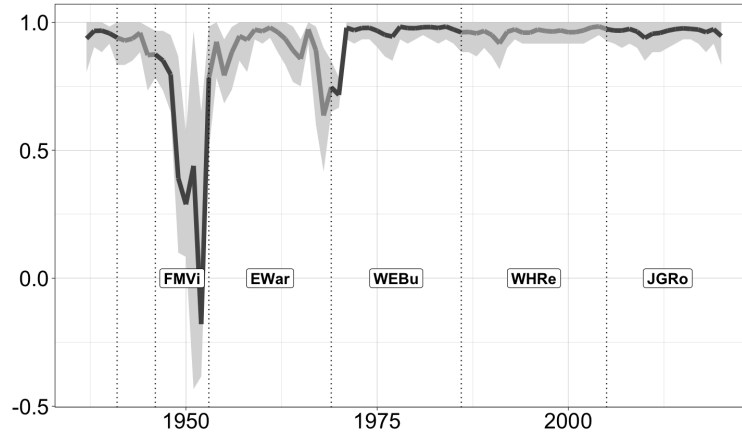


Fig. 7: Posterior mean (solid line) and 95% credible intervals for the ideal points of justices William Douglas, justice Hugo Black and Felix Frankfurter. The left column displays estimates based on our circular model, whereas the right column displays the MQ scores. Zero is indicated by a dashed line and $\pm\pi$ by a dotted line.

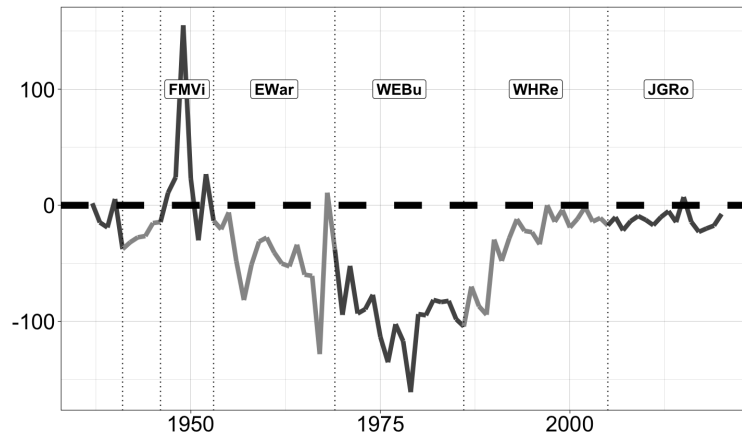
5. A case study: The evolution of justices' preferences in the U.S. Supreme Court

In this Section, we analyze the data introduced in Section 2 using the circular model described in this paper, and compare the results of the analysis with those obtained using the methodology of Martin and Quinn (2002) (in the sequel, MQ) as implemented in the R package `mcmcPack` (Martin et al., 2011). Results for our model are based on 40,000 samples of the posterior distribution obtained from the algorithm described in Section 4 after thinning the original chain every 25 observations. Results for the MQ model are based on 40,000 posterior samples.

Figures 6 and 7 show the estimated trajectories of the ideal points of eight justices with relatively long tenures under our circular (left column) and the MQ (right column) models. The trajectories for the five justices included in Figure 6 are very similar under both models. These similarities are representative of the results for most (but not all!) of the 48 justices in the dataset. In contrast, Figure 7 shows three examples of judges for which the estimated trajectories of the ideal points arising from our circular model are qualitatively different from those that arise under the MQ model. The most striking difference is for Justice Hugo Black. While the MQ model suggests that Black started a liberal who tended to moderate his positions over time to become a centrist, the circular model suggests a much more stable (and extreme) behavior characterized by a mostly liberal ideology punctuated by crosses towards the conservative side of the ideological spectrum (through the lower pole) in 1952 term and the 1969-1970 terms. Similarly, the MQ model has Justice William Douglas becoming increasingly more liberal starting in 1960, while our circular model yields a stable ideological profile. Finally, while the overall shape of Justice Felix Frankfurter's trajectory is similar across both models and reflect increasing conservative leanings in his voting patters, the circular model identifies a couple of drops in the 1951 and 1953-1954 terms that are not



(a) Spearman correlation among ranks



(b) Difference in WAIC between circular and MQ models

Fig. 8: Top plot shows the posterior mean (solid line) and corresponding 95% credible intervals (shaded region) for the Spearman correlation between the justices' rankings generated by the circular and the MQ models. The bottom plot shows the difference between the WAIC computed for the MQ and circular models. Here, a negative difference indicates that MQ is preferred whereas a positive difference indicates the circular model is preferred.

present in the MQ scores. While the qualitative differences between the trajectories estimated by both models are restricted to a relatively small number of justices, they can have important consequences for our understanding of the Court's dynamics (please see Sections 5.1 and 5.2).

Additional insight into the differences between both models can be obtained by comparing the justices' ideological rankings. Figure 8a presents the posterior mean and associated 95% credible intervals for the Spearman correlation among the justices' ranks (e.g., see Kumar and Vassilvitskii, 2010) generated by the circular and MQ models. Starting in 1975, the posterior distribution of this metric has been highly concentrated around 1, indicating that the MQ and circular models lead to identical ideological rankings of the justices. However, before 1975, there are various periods of time in which the rankings disagree, in some cases quite strongly. Interestingly, these periods have tended to coincide with changes in Chief Justice, particularly the transition from Fred M. Vinson to Earl Warren, and the the following one from Earl Warren to Warren E. Burger.

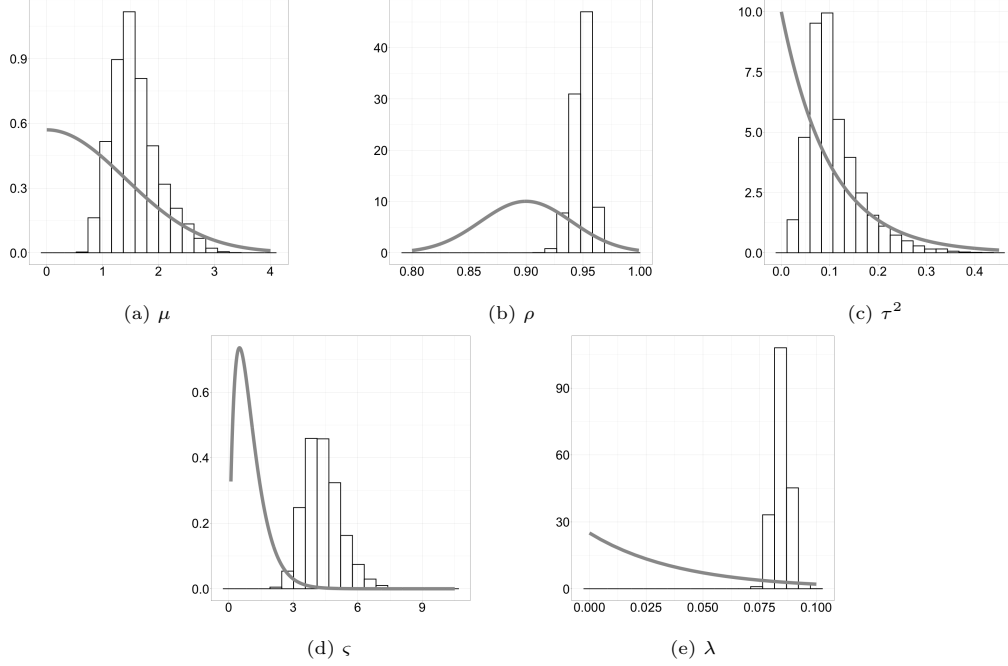


Fig. 9: Histogram of the posterior distribution of various hyperparameters. Solid lines correspond to the respective prior distributions.

In order to assess the relative validity of the models during these periods of disagreement in the ideological ranking, we investigate model fit using the Watanabe-Akaike Information Criterion (WAIC, Watanabe and Opper, 2010, Watanabe, 2013, Gelman et al., 2014). Similarly to the well-known Akaike information criteria (AIC) and the Bayesian information criteria (BIC), WAIC balances goodness of fit against model complexity. However, unlike the AIC and the BIC, the WAIC is well suited for hierarchical models where the number of effective parameters can be much smaller than the headline number. Compared to the deviance information criteria (DIC), the WAIC has the additional advantage of being invariant to reparameterizations of the model (Gelman et al., 2014; Spiegelhalter et al., 2014). We compute the WAIC for model m during period t from the output of the Markov chain Monte Carlo algorithms as:

$$WAIC_t(m) = \sum_{i=1}^I \log \left(E_{\text{post}} \left\{ \prod_j \theta_{i,j,t}(m)^{y_{i,j,t}} [1 - \theta_{i,j,t}(m)]^{1-y_{i,j,t}} \right\} \right) - \sum_{i=1}^I \text{var}_{\text{post}} \left\{ \sum_j [y_{i,j,t} \log \theta_{i,j,t}(m) + (1 - y_{i,j,t}) \log(1 - \theta_{i,j,t}(m))] \right\}, \quad (9)$$

where $E_{\text{post}}\{\cdot\}$ and $\text{var}_{\text{post}}\{\cdot\}$ denote the mean and variances computed over the posterior distribution, and $\theta_{i,j,t}(m)$ represents the probability that justice i votes to reverse the lower court decision on case j during term t under model m . Figure 8b presents the difference between the value of the WAIC for the circular model and that for the MQ model, $WAIC_t(C) - WAIC_t(MQ)$, so that positive values favor our circular model, and viceversa. Note that periods in which the rankings generated by the circular model disagree with those of the Euclidean model are also periods where the WAIC indicates that the circular model provides a better fit for the data, even after adjusting for its additional complexity. The graph also indicates that, while the MQ model is strongly preferred during the Burger court, its advantage starts to erode after William Rehnquist's appointment as Chief Justice. Indeed, during the second half of Rehnquist's and during all of John Roberts' tenure as Chief Justices,

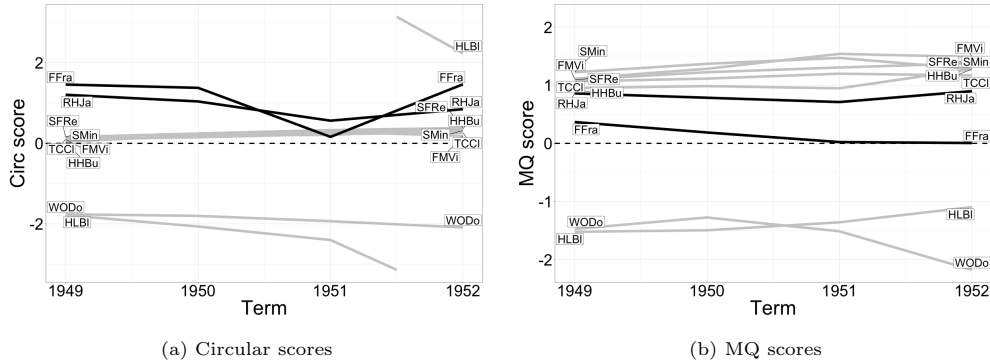


Fig. 10: Plots displaying the circular scores of justices on the Supreme Court from 1949 to 1952 on the left and Martin Quinn scores of the same justices on the right. The ideology trajectories of justices Felix Frankfurter and Robert Jackson are highlighted.

the evidence in favor of the MQ model has been relatively weak, with our circular model being preferred during some terms.

Finally, Figure 9 displays histograms of posterior samples of the hyperparameters μ , ρ , τ^2 , ζ and λ . Notice that all posteriors are unimodal with potentially some skew to the right. With the exception of τ^2 , the posteriors are shifted to the right of the prior distribution. For instance, the posterior mean of ρ changes from 0.9 to 0.95. Furthermore, the posteriors of λ and ρ are particularly concentrated compared to their respective prior distribution. Meanwhile, the posterior of μ is slightly more concentrated compared to its prior whereas the posterior of ζ is slightly less concentrated.

We look now in more detail at the results for the two periods where our circular model seems to dominate the MQ model, 1949–1952 and 1967–1970.

5.1. Supreme Court ideology, 1949–1952

The early and mid 1930s were a period of increasing conflict between the executive and judicial branches of the U.S. Federal Government. Put briefly, this conflict was driven by repeated instances of a (“conservative”) Supreme Court bent on protecting property rights striking down “New Deal” legislation put forward by the (“liberal”) administration of Franklin D. Roosevelt to address the causes and consequences of the Great Recession. By 1941, however, the conflict had been resolved by the fact that Roosevelt had been able to name all nine members of SCOTUS. By the 1949 term, the Court composition had changed again. Five Roosevelt appointees remained in the court (Justices Felix Frankfurter, Robert Jackson, Hugo Black, William O. Douglas and Stanley F. Reed), joined by four recent Truman appointees (Justices Harold H. Burton, Fred M. Vinson, Tom C. Clark and Sherman Minton, with Clark and Minton in their first term).

While Frankfurter, Jackson, Black and Douglas started their appointments in the Court with similar liberal political inclinations and were committed New Dealers named to SCOTUS by Roosevelt, once on the bench, they developed radically different judicial philosophies and strained interpersonal relationships that often put them at odds with each other. Before joining the court, Frankfurter was a staunch supporter of liberal political ideas and one of the founders of the American Civil Liberties Union. However, during his tenure as justice, he became the Court’s most outspoken advocate of judicial restraint, the view that courts should not interpret the constitution in such a way as to impose sharp limits upon the authority of the legislative and executive branches (Irons, 2006). He also had a pompous style that strained his personal relationship with other justices. Many historians have come to see Frankfurter as the eventual leader of the conservative faction of the Supreme Court (e.g., see Eisler and Eisler, 1993), to which Jackson (a frequent ally of Frankfurter, specially in his animosity towards justices Douglas and Black) also belonged. Black was also an adherent of judicial restraint (specially during the early part of his tenure on the Court), but he was also a committed literalist and absolutist who disliked and repeatedly clashed with Frankfurter and Jackson (Ball, 1996; Magee, 1980). Finally, Douglas espoused a pragmatic judicial

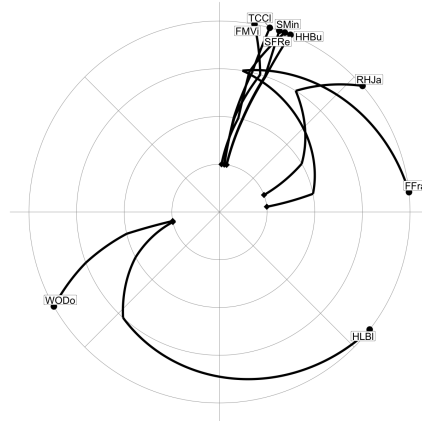


Fig. 11: Circular scores of justices on the Supreme Court from 1949 to 1952 on a (more appropriate) polar scale.

philosophy that did not highly value judicial consistency when deciding cases and relied on philosophical insights and observations about current politics as much as more conventional judicial sources (Tomlins et al., 2005) .

With this background in mind, we now focus on the trajectories of the ideal points of the nine SCOTUS justices from 1949 to 1952 (see Figure 10). We can see in Figure 10b that the MQ model places both Frankfurter and Jackson as centrists, or even liberals. In fact, the MQ model makes them seem like the two judges whose ideal points are closest to those of Douglas and Black. This is clearly at odds with the consensus historical analysis that we described before, especially as it relates to Frankfurter’s ideology. In contrast, the circular model places both Frankfurter and Jackson to the right of Truman’s appointees, and Black and Douglas to their left.

While the circular model seems to lead to a more realistic ranking of justices during this period, this example also can be seen as a warning against trying to use a circular geometry to infer preferences on a liberal-conservative scale. Under a circular geometry, Douglas and Black are not really on opposite ends of the spectrum from Frankfurter and Jackson. Their ideologies connect through the bottom of the circle, as evidenced by the fact that, in 1952, Black’s ideal point is in fact positive and close to those of Frankfurter and Jackson. Hence, it is better to interpret the circular model as suggesting the presence of three groups of justices: one made of all Truman appointees plus Justice Reed, another made of Douglas and Black, and a third made of Frankfurter and Jackson, roughly lined up as the vertices of a triangle (please see Figure 11). Outcomes on specific cases are driven by ad-hoc alliances among justices that often come from all three groups. Such three-ways alliances, which have low-probability under the MQ model, are much more likely under the circular geometry. This shows that the circular model, while remaining one-dimensional in principle, allows for a richer characterization of the interactions among justices than what is possible using a Euclidean latent space.

We believe that the dominance of the circular model during this particular period of the court can be explained in part by shifting views on the doctrine of judicial restraint. As discussed in Feldman (2010), judicial restraint had been favored judicial philosophy among liberal lawyers and justices during the 1920s and the 1930s, as it served as check on what they saw as an overly conservative SCOTUS. With the changes to the Court composition occurring during the Roosevelt years, judicial restraint acted as a brake on the ambitions of liberal justices, most of whom had come to SCOTUS with clear political ambitions and after serving in the legislative and executive branches rather than in academia or the courts. As they settled on their positions in the Court, several of Roosevelt’s appointees either ditched judicial restraint completely, or applied it selectively depending on whether the consequences on a particular case agreed with their political goals. This explains how Justice Felix Frankfurter, by holding on to judicial restraint as the guiding principle of his jurisprudence, became known as the leader of the “conservative” wing of the Court, and Douglas and Black as defendants of “liberalism”, while still being able to vote together on a number nonunanimous decisions.

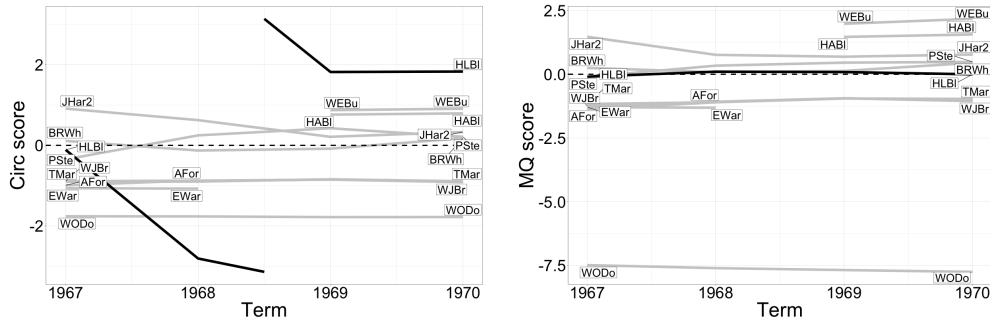


Fig. 12: Plots displaying the circular scores of justices on the Supreme Court from 1968 to 1970 on the left and Martin Quinn scores of the same justices on the right. The ideology trajectories of justices Hugo Black are highlighted.

5.2. Supreme Court ideology, 1967–1970

The 1967–1970 period covers the last two years of the Warren Court and the first two of the Burger Court. Both courts are considered by historians as strongly liberal. The Warren court in particular is famous for expanding civil rights, civil liberties and judicial power in dramatic ways.

Figure 12 shows the trajectories of the ideal points of all the justices that served in the Court during this period. It is clear from the plots that the main discrepancy between the two models refers to the estimates associated with justice’s Black preferences. Under the MQ model, Black appears to be a relative moderate during this period. This is at odds with the opinion of various experts. Indeed, while Black was considered a liberal during the early part of his tenure in the Court, towards the end of his career, his “originalism was turning him into a judicial split personality: now liberal, now conservative” (Feldman, 2010). Black opposed the Warren Court’s expansion of civil liberties, as he did not believe that the original text of the Constitution supported this expansion, except in the case of free speech. This understanding of Black’s ideology agrees much more closely with the estimates generated by the circular model.

5.3. Sensitivity Analysis

To investigate the sensitivity of the results to the choice of priors, we repeated our analyses using an alternative set of priors in which ρ is assigned a Gaussian distribution with mean 0.95, standard deviation 0.05 which was truncated to the $[0, 1]$ interval (this implies $\Pr(0.85 < \rho < 1) \approx 0.975$ a priori), μ was assigned another Gaussian distribution with mean 10, standard deviation 5, and truncated to the positive reals, τ^2 was assigned an exponential prior with mean 0.5, and $1/\lambda$ another exponential distribution with mean 7.9. The prior on ς remained the same (a Gamma distribution with mean 1 and variance 0.5). The implied prior on $\beta_{i,t}$ is more concentrated than the one we used for our original analysis, while the implied prior on $\theta_{i,j,t}$ is still trimodal, but less peaked at 0 and 1. Please see Section 3 of the supplementary materials for a visual representation of these two implied priors.

The results appear to be reasonably robust to our choice of priors, although there are some small differences. In particular, while the posterior distribution of the hyperparameters ρ , ς and λ remain the same, the posterior distributions for μ and τ^2 seem to favor slightly higher values under our alternative priors. On the other hand, the trajectories of a couple of the justices’ ideologies seem to be slightly smoother under our alternative prior. However, the key conclusions from our previous analyses do not seem to be affected by the new priors. Please see the supplementary materials for additional details.

6. Discussion

This paper introduces a novel dynamic factor model for binary data that relies on a circular latent space. The model is motivated by the problem of assessing the evolution of the ideological preferences of U.S. Supreme Court justices. We show that the circular model replicates the results of more traditional Euclidean voting

models when the data supports such models, while providing a richer and more accurate description of the justices' behavior at key historical periods in which the results from traditional Euclidean models contradict well-established narratives around legislator's ideology. In particular, our results suggest that a circular policy space might be more appropriate during the Vinson court, and possibly during the transition between the Warren and Burger courts. Our results also indicate that, starting in the mid 90s, both Euclidean and circular models have performed quite similarly.

Our circular model suffers from many of the same shortcomings as other factor models used for scaling preferences, including the one proposed by Martin and Quinn (2002). In particular, a key assumption that is rarely explicitly acknowledged is that the distribution of the decision-specific parameters $(\psi_{i,t}, \zeta_{i,t})$ remains constant over time. Because the SCOTUS justices can select the cases they will consider in a given term, this assumption is suspect in our application. In other words, it is possible that some of the fluctuations in ideal points capture by these models might be due to changes in the nature of the cases in SCOTUS' docket rather than a reflection of changing ideology among justices. In our application, this shortcoming might be particularly impactful starting in the mid-90s, when the number of SCOTUS decisions drops dramatically and. Interestingly, this is the same time frame in which the differences in performance between the circular and the Euclidean models shrinks substantially.

Parameter estimation for our circular factor model relied on the use of an elliptical slice sampler for sampling each of the trajectories β_1, \dots, β_I . While this algorithm is fairly straightforward to implement, it can mix poorly. Hence, accurate posterior inference can be computationally expensive, requiring a large number of posterior samples. In the future, we aim to explore alternative computational strategies based on blockwise Hamiltonian Monte Carlo steps to update justice's ideal point trajectories. Other plausible extensions that will be considered in the future include dynamic models that rely on higher-dimensional spherical policy spaces, as well as models based on more general latent geometries.

Acknowledgements

We would like to thank Kevin Quinn for his help with the R package `mcmcPack`.

References

- Angelopoulos, J., Sahoo, S. and Visvikis, I. D. (2020) Commodity and transportation economic market interactions revisited: new evidence from a dynamic factor model. *Transportation Research Part E: Logistics and Transportation Review*, **133**, 101836.
- Bailey, M. A. (2007) Comparable preference estimates across time and institutions for the court, congress, and presidency. *American Journal of Political Science*, **51**, 433–448.
- Bailey, M. A., Strezhnev, A. and Voeten, E. (2017) Estimating dynamic state preferences from united nations voting data. *Journal of Conflict Resolution*, **61**, 430–456.
- Ball, H. (1996) *Hugo L. Black: cold steel warrior*. Oxford University Press on Demand.
- Barhoumi, K., Darné, O. and Ferrara, L. (2013) Dynamic factor models: A review of the literature. *Available at SSRN 2291459*.
- Bellégo, C. and Ferrara, L. (2012) Macro-financial linkages and business cycles: A factor-augmented probit approach. *Economic Modelling*, **29**, 1793–1797.
- Bertomeu, J. G., Dalla Pellegrina, L. and Garoupa, N. (2017) Estimating judicial ideal points in latin america: the case of argentina. *Review of Law & Economics*, **13**.
- Black, R. C. and Owens, R. J. (2009) Agenda setting in the supreme court: The collision of policy and jurisprudence. *The Journal of Politics*, **71**, 1062–1075.
- Casillas, C. J., Enns, P. K. and Wohlfarth, P. C. (2011) How public opinion constrains the us supreme court. *American Journal of Political Science*, **55**, 74–88.
- Cattell, R. (2012) *The scientific use of factor analysis in behavioral and life sciences*. Springer Science & Business Media.
- Crane, H. (2017) A hidden markov model for latent temporal clustering with application to ideological alignment in the us supreme court. *Computational Statistics & Data Analysis*, **110**, 19–36.
- Davis, O. A., Hinich, M. J. and Ordeshook, P. C. (1970) An expository development of a mathematical model of the electoral process. *American political science review*, **64**, 426–448.

- Duck-Mayr, J. and Montgomery, J. (2022) Ends against the middle: Measuring latent traits when opposites respond the same way for antithetical reasons. *Political Analysis*, 1–20.
- Eisler, K. I. and Eisler, K. T. (1993) *A Justice for All: William J. Brennan, Jr., and the decisions that transformed America*. Simon & Schuster.
- Embretson, S. E. and Reise, S. P. (2013) *Item response theory*. Psychology Press.
- Enders, C. K. (2010) *Applied missing data analysis*. Guilford press.
- Enelow, J. M. and Hinich, M. J. (1984) *The spatial theory of voting: An introduction*. CUP Archive.
- Epstein, L., Martin, A. D., Segal, J. A. and Westerland, C. (2007) The judicial common space. *The Journal of Law, Economics, and Organization*, **23**, 303–325.
- Feldman, N. (2010) *Scorpions: the battles and triumphs of FDR's great Supreme Court justices*. New York: Twelve, 1st edn. OCLC: ocn528665984.
- Forni, M., Hallin, M., Lippi, M. and Reichlin, L. (2000) The generalized dynamic-factor model: Identification and estimation. *Review of Economics and Statistics*, **82**, 540–554.
- Fountas, G., Sarwar, M. T., Anastasopoulos, P. C., Blatt, A. and Majka, K. (2018) Analysis of stationary and dynamic factors affecting highway accident occurrence: a dynamic correlated grouped random parameters binary logit approach. *Accident Analysis & Prevention*, **113**, 330–340.
- Fox, J.-P. (2010) *Bayesian item response modeling: Theory and applications*. Springer.
- Gelman, A., Hwang, J. and Vehtari, A. (2014) Understanding predictive information criteria for bayesian models. *Statistics and computing*, **24**, 997–1016.
- Harvard Law Review (2022) SCOTUS Statistics - Harvard Law Review. URL: <https://harvardlawreview.org/supreme-court-statistics/>.
- Irons, P. (2006) *A People's History of the Supreme Court: The Men and Women Whose Cases and Decisions Have Shaped Our Constitution: Revised Edition*. Penguin.
- Jackman, S. (2001) Multidimensional analysis of roll call data via bayesian simulation: Identification, estimation, inference, and model checking. *Political Analysis*, **9**, 227–241.
- Kovac, M. et al. (2019) Replicating and extending martin-quinn scores. *International Review of Law and Economics*, **60**, 105861.
- Kumar, R. and Vassilvitskii, S. (2010) Generalized distances between rankings. In *Proceedings of the 19th international conference on World wide web*, 571–580.
- Lepore, J. (2014) The Cold Case of Justice Felix Frankfurter's Stolen Papers. *The New Yorker*. URL: <https://www.newyorker.com/magazine/2014/12/01/great-paper-caper>. Section: american chronicles.
- Linzer, D. A. and Staton, J. K. (2015) A global measure of judicial independence, 1948–2012. *Journal of Law and Courts*, **3**, 223–256.
- Lo, J. (2018) Dynamic ideal point estimation for the european parliament, 1980–2009. *Public Choice*, **176**, 229–246.
- Magee, J. J. (1980) *Mr. Justice Black, Absolutist on the Court*. University of Virginia Press.
- Mardia, K. V., Jupp, P. E. and Mardia, K. (2000) *Directional statistics*, vol. 2. Wiley Online Library.
- Martin, A. D. and Quinn, K. M. (2002) Dynamic ideal point estimation via markov chain monte carlo for the us supreme court, 1953–1999. *Political analysis*, **10**, 134–153.
- Martin, A. D., Quinn, K. M. and Park, J. H. (2011) MCMCpack: Markov chain monte carlo in R.
- McFadden, D. (1973) Conditional logit analysis of qualitative choice behavior. In *Frontiers in Econometrics* (ed. P. Zarembka), 105–142. New York: Academic.
- Mokken, R. J., van Schuur, W. H. and Leeferink, A. J. (2001) The circles of our minds: A nonparametric irt model for the circumplex. In *Essays on item response theory*, 339–356. Springer.
- Murray, I., Adams, R. P. and MacKay, D. J. C. (2010) Elliptical slice sampling. *Proceedings of the 13th International Conference on Artificial Intelligence and Statistics (AISTATS) (JMLR: W&CP)*, **6**, 8.
- Owens, R. J. and Wedeking, J. P. (2011) Justices and legal clarity: Analyzing the complexity of us supreme court opinions. *Law & Society Review*, **45**, 1027–1061.
- Paganin, S., Paciorek, C. J., Wehrhahn, C., Rodríguez, A., Rabe-Hesketh, S. and de Valpine, P. (2022) Computational strategies and estimation performance with bayesian semiparametric item response theory models. *Journal of Educational and Behavioral Statistics*, 10769986221136105.
- Peña, D. and Poncela, P. (2004) Forecasting with nonstationary dynamic factor models. *Journal of Econometrics*, **119**, 291–321.

- Poole, K. T. and Rosenthal, H. (1985) A spatial model for legislative roll call analysis. *American journal of political science*, 357–384.
- Reise, S. and Rodriguez, A. (2016) Item response theory and the measurement of psychiatric constructs: some empirical and conceptual issues and challenges. *Psychological Medicine*, **46**, 2025–2039.
- Roberts, J. S., Donoghue, J. R. and Laughlin, J. E. (2000) A general item response theory model for unfolding unidimensional polytomous responses. *Applied Psychological Measurement*, **24**, 3–32.
- Rodriguez, A. and Moser, S. (2015) Measuring and accounting for strategic abstentions in the us senate, 1989–2012. *Journal of the Royal Statistical Society: Series C (Applied Statistics)*, **64**, 779–797.
- Rohde, D. W. and Spaeth, H. J. (1976) *Supreme court decision making*. Political science. San Francisco: Freeman.
- Rummel, R. J. (1988) *Applied factor analysis*. Northwestern University Press.
- Schubert, G. (1965) *The Judicial Mind: The Attitudes and Ideologies of Supreme Court Justices 1946-1963*. Evanston: Northwestern University Press. URL: <https://openyls.law.yale.edu/handle/20.500.13051/15219>. Accepted: 2021-11-26T12:22:52Z.
- Segal, J. A. and Cover, A. D. (1989) Ideological values and the votes of us supreme court justices. *American Political Science Review*, **83**, 557–565.
- Small, C. G. (2012) *The statistical theory of shape*. Springer Science & Business Media.
- Spiegelhalter, D. J., Best, N. G., Carlin, B. P. and Van der Linde, A. (2014) The deviance information criterion: 12 years on. *Journal of the Royal Statistical Society: Series B: Statistical Methodology*, 485–493.
- Spirling, A. and Quinn, K. (2010) Identifying intraparty voting blocs in the uk house of commons. *Journal of the American Statistical Association*, **105**, 447–457.
- Stock, J. H. and Watson, M. W. (2016) Dynamic factor models, factor-augmented vector autoregressions, and structural vector autoregressions in macroeconomics. In *Handbook of macroeconomics*, vol. 2, 415–525. Elsevier.
- Thomas, M. L. (2011) The value of item response theory in clinical assessment: a review. *Assessment*, **18**, 291–307.
- Tomlins, C. L. et al. (2005) *The United States Supreme Court: The Pursuit of Justice*. Houghton Mifflin Harcourt.
- Wang, F. and Gelfand, A. E. (2014) Modeling space and space-time directional data using projected gaussian processes. *Journal of the American Statistical Association*, **109**, 1565–1580.
- Watanabe, S. (2013) A widely applicable bayesian information criterion. *The Journal of Machine Learning Research*, **14**, 867–897.
- Watanabe, S. and Opper, M. (2010) Asymptotic equivalence of bayes cross validation and widely applicable information criterion in singular learning theory. *Journal of machine learning research*, **11**.
- Weisberg, H. F. (1974) Dimensionland: An excursion into spaces. *American Journal of Political Science*, 743–776.
- Yu, X. and Rodríguez, A. (2021) Spatial voting models in circular spaces: A case study of the us house of representatives. *The Annals of Applied Statistics*, **15**, 1897–1922.

Supplementary Material for “Dynamic Factor Models for Binary Data in Circular Spaces: An Application to the U.S. Supreme Court”

Rayleigh Lei and Abel Rodriguez

1 Interpretation of the parameters of the circular autoregressive process

Figure 1 presents histograms based on 10,000 samples from the marginal distribution of a circular autoregressive process defined in Section 3.1 of the main manuscript for various combinations of (fixed) hyperparameters. Because $\mu_2 = 0$ in all cases, the mean of all the distributions is zero. From these plots, it can be seen that lower values of ρ lead reduce the variance of the stationary distribution (see Figure 1b). On the other hand, either lower values of μ_1 or higher values of τ_1 or τ_2 lead to distributions with higher marginal variance. Note however, that while μ_1 seems to only affect the variance (Figure 1c), τ_1 or τ_2 also affect the shape of the marginal distribution in other ways. In particular, when the ratio τ_1/τ_2 becomes either much larger or much smaller than one, the distribution becomes first platykurtic (as in Figure 1d) and eventually bimodal (as in Figure 1e and 1f). Note that when τ_1/τ_2 is much larger than one, the two modes of the distribution of angles are located at $\beta_{i,t} = 0$ and $\beta_{i,t} = \pi$. On the other hand, when τ_1/τ_2 is much smaller than 1, the two modes are symmetric around $\beta_{i,t} = 0$, but clearly away from it.

2 Computation

We fit our model using a Gibbs sampler. We sampled for $\psi_{j,t}$, $\zeta_{j,t}$, \mathbf{v}_i , and \mathbf{w}_i for $i = 1, 2, \dots, I$, $t = 1, 2, \dots, T$, and $j = 1, 2, \dots, J_t$. Set $\beta_{i,t} = \arctan 2(z_{i,t,1}, z_{i,t,2})$ where $\arctan 2(\cdot, \cdot)$ is defined in (5) from the main manuscript. Then, the steps are the following:

- For $\psi_{j,t}, \zeta_{j,t} \mid \beta_{i,t}, \kappa_j$, $i = 1, 2, \dots, I$, $t = 1, 2, \dots, T$, and $j = 1, 2, \dots, J_t$, propose $\psi'_{j,t}, \zeta'_{j,t}$ using Hamiltonian Monte Carlo. However, we use the following function instead for our momentum: $K(\mathbf{m}) = -c_1 \cos(m_1) - c_2 \cos(m_2)$. In other words, we’re using an independent von Mises kernel for our momentum vectors. Then, the gradients for the momentum vector are $(c_1 \sin(m_1), c_2 \cos(m_2))^T$. Meanwhile, because the likelihood is

$$L(\psi_{j,t}, \zeta_{j,t}) := \prod_{i=1}^I \text{Bern}(y_{i,j,t} \mid \theta_{i,j,t}) \mathbb{I}(y_{i,j,t} \in \{0, 1\}),$$

the gradients for the likelihood with respect to $\psi_{j,t}$ and $\zeta_{j,t}$ are given in the following subsection. Here,

$$\theta_{i,j,t} = G_{\kappa_{j,t}} \left(\left\{ \arccos(\cos(\zeta_{j,t} - \beta_{i,t})) \right\}^2 - \left\{ \arccos(\cos(\psi_{j,t}, \beta_{i,t})) \right\}^2 \right).$$

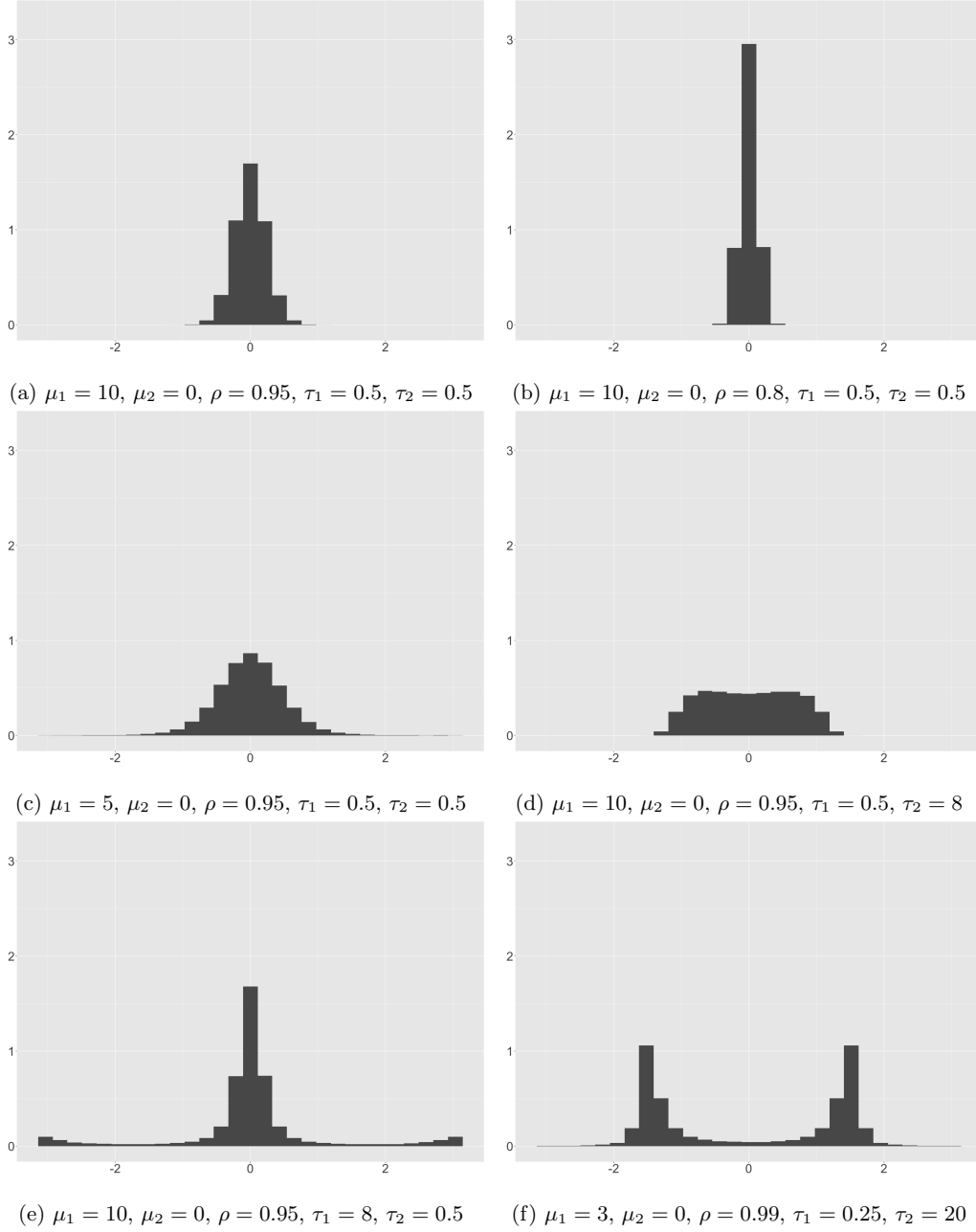


Figure 1: Plots showing 10,000 draws from the marginal prior distribution for $\beta_{i,t}$ according to various hyperpriors.

Then, we accept the proposal with the following probability:

$$\min(1, \exp(L(\psi'_{j,t}, \zeta'_{j,t}) - L(\psi_{j,t}, \zeta_{j,t}) - c_1 \cos(m'_1) - c_2 \cos(m'_2) + c_1 \cos(m_1) + c_2 \cos(m_2))). \quad (1)$$

- For $\mathbf{v}_i, \mathbf{w}_i \mid \psi_{j,t}, \zeta_{j,t}, \kappa_j, \mu, \tau, \varsigma, \rho$, propose a new vector using elliptical slice sampling. Set

$$\mathbf{Z}_i = \begin{pmatrix} z_{i,1,1} & z_{i,1,2} \\ z_{i,2,1} & z_{i,2,2} \\ \vdots & \vdots \\ z_{i,T,1} & z_{i,T,2} \end{pmatrix} = \begin{pmatrix} v_{i,1} - \mu & w_{i,1} \\ v_{i,2} - \mu & w_{i,2} \\ \vdots & \vdots \\ v_{i,T_i} - \mu & w_{i,T_i} \end{pmatrix}$$

and focus on sampling \mathbf{Z}_i from its full conditional distribution

$$p(\mathbf{Z}_i \mid \dots) \propto \exp \left\{ -\frac{1}{2\tau^2} \text{tr} [\boldsymbol{\Sigma} \mathbf{Z}_i^T \boldsymbol{\Omega}(\rho) \mathbf{Z}_i] \right\} \prod_{t=1}^T \prod_{j=1}^{J_t} \{\theta(z_{i,t,1}, z_{i,t,2})\}^{y_{i,j}} \{1 - \theta(z_{i,t,1}, z_{i,t,2})\}^{y_{i,j}},$$

where $\boldsymbol{\Sigma} = \text{diag}\{1, 1/\varsigma\}$, $\boldsymbol{\Omega}(\rho)$ is defined in (7) from the main manuscript, and

$$\theta(z_{i,t,1}, z_{i,t,2}) = G_{\kappa_{j,t}} \left(\left\{ \arccos(\cos(\zeta_{j,t} - \text{atan2}(z_{i,t,1} + \mu, z_{i,t,2}))) \right\}^2 - \left\{ \arccos(\cos(\psi_{j,t} - \text{atan2}(z_{i,t,1} + \mu, z_{i,t,2}))) \right\}^2 \right).$$

Then, draw a an auxiliary matrix \mathbf{U}^* from a matrix normal distribution

$$\mathbf{U}^* \mid \tau^2, \varsigma, \rho \sim \text{MN}(\mathbf{U}^* \mid \mathbf{0}, \boldsymbol{\Omega}^{-1}(\rho), \tau^2 \boldsymbol{\Sigma}^{-1})$$

along with a random threshold $c \sim \text{Unif}[0, 1]$ and a random angle $a \sim \text{Unif}[0, 2\pi)$. Set $a_{\min} = a - 2\pi$ and $a_{\max} = a$. A proposal for \mathbf{Z}_i is then generated as $\mathbf{Z}_i^* = \cos(a)\mathbf{Z}_i + \sin(a)\mathbf{U}^*$, and this proposal accepted if

$$\frac{\prod_{t=1}^T \prod_{j=1}^{J_t} \{\theta(z_{i,t,1}^*, z_{i,t,2}^*)\}^{y_{i,j}} \{1 - \theta(z_{i,t,1}^*, z_{i,t,2}^*)\}^{y_{i,j}}}{\prod_{t=1}^T \prod_{j=1}^{J_t} \{\theta(z_{i,t,1}, z_{i,t,2})\}^{y_{i,j}} \{1 - \theta(z_{i,t,1}, z_{i,t,2})\}^{y_{i,j}}} > c.$$

If the proposal \mathbf{Z}_i^* is rejected, set $a_{\min} = a$ if $a < 0$ and $a_{\max} = a$ if $a \geq 0$. Then, draw a from $\text{Unif}(a_{\min}, a_{\max})$. Propose a new \mathbf{Z}_i^* with this new a and check whether to accept this proposal. If the proposal is still rejected, repeat this process until either the proposal is accepted or the support for a becomes empty.

In addition, we sample for the hyperparameters in the following manner. We sampled $\{\kappa_j\}_{j=1}^J$ using a random walk on the log scale. The acceptance probability for a new κ'_j given κ_j is the following:

$$\frac{\prod_{i=1}^I \text{Bern}(y_{i,j,t} \mid \theta'_{i,j,t}) \mathbb{I}(y_{i,j,t} \in \{0, 1\}) \exp(\kappa'_j \mid \lambda_\kappa) \kappa'_j}{\prod_{i=1}^I \text{Bern}(y_{i,j,t} \mid \theta_{i,j,t}) \mathbb{I}(y_{i,j,t} \in \{0, 1\}) \exp(\kappa_j \mid \lambda_\kappa) \kappa_j}.$$

Here,

$$\theta'_{i,j,t} = G_{\kappa'_{j,t}} \left(\left\{ \arccos(\cos(\zeta_{j,t} - \beta_{i,t})) \right\}^2 - \left\{ \arccos(\cos(\psi_{j,t}, \beta_{i,t})) \right\}^2 \right).$$

Meanwhile, we can draw $\lambda_\kappa \mid \{\kappa_j\}_{j=1}^J$ from the following distribution if we use an exponential distribution with mean m_λ :

$$\lambda_\kappa \propto \Gamma \left(1 + J, \frac{1}{m_\lambda} + \sum_{j=1}^J \kappa_j \right). \quad (2)$$

For $\mu, \tau^2, \varsigma, \rho$, the likelihood only involves \mathbf{v}_i and \mathbf{w}_i from above. We sampled μ, τ^2, ς with a random walk on the log scale because they are highly correlated. A new $\tau'^2, \varsigma', \mu'$ given $\rho, \mathbf{v}_i, \mathbf{w}_i$ for $i = 1, 2, \dots, I$, and a previous τ^2, ς, μ is accepted with the following probability:

$$\frac{\prod_{i=1}^I \text{MN}((\mathbf{v}_i; \mathbf{w}_i) | (\mu' \mathbf{1}_{T_i}; \mathbf{0}_{T_i}), \mathbf{\Omega}^{-1}(\rho), \tau'^2 \mathbf{\Sigma}'^{-1}) p(\tau', \varsigma', \mu') \tau'^2 \varsigma' \mu'}{\prod_{i=1}^I \text{MN}((\mathbf{v}_i; \mathbf{w}_i) | (\mu \mathbf{1}_{T_i}; \mathbf{0}_{T_i}), \mathbf{\Omega}^{-1}(\rho), \tau^2 \mathbf{\Sigma}^{-1}) p(\tau, \varsigma, \mu) \tau^2 \varsigma \mu}, \quad (3)$$

where

$$p(\tau, \varsigma, \mu) = \exp\left(\tau'^2 \mid \frac{1}{m_\lambda}\right) \Gamma(\varsigma \mid a_\varsigma, b_\varsigma) \text{N}_{(0, \infty)}(\mu \mid m_\mu, s_\mu^2).$$

and $(A; B)$ denotes a matrix $M \in \mathbb{R}^{N \times 2}$ such that $\mathbf{M}_{\cdot, 1} = A$ and $\mathbf{M}_{\cdot, 2} = B$.

Finally, we sample for ρ in the following manner.

- Set

$$\begin{aligned} \tilde{m}_\rho &= \frac{1}{\tau} \sum_{i=1}^I \mathbb{I}(T_i > 1) \sum_{t=1}^{T_i-1} ((v_{i,t+1} - \mu)(v_{i,t} - \mu)) + \frac{1}{\varsigma} (w_{i,t+1} w_{i,t}), \\ \tilde{s}_\rho^2 &= \frac{1}{s_\rho^2} + \frac{1}{\tau} \sum_{i=1}^I \sum_{t=1}^{T_i-1} (v_{i,t} - \mu)^2 + \frac{1}{\varsigma} (w_{i,t})^2. \end{aligned}$$

Draw ρ' from the following distribution,

$$\tilde{\rho} \propto \text{N}\left(\cdot \mid \frac{\tilde{m}_\rho}{\tilde{s}_\rho^2}, \frac{1}{\tilde{s}_\rho^2}\right) \mathbb{I}(-0 < \tilde{\rho} < 1) \quad (4)$$

- Accept ρ' with the following probability:

$$\min\left(\left(\frac{1 - (\rho')^2}{1 - \rho^2}\right)^I \exp\left(\frac{(\rho')^2 - \rho^2}{2\tau^2} \sum_{i=1}^I (v_{i,1} - \mu)^2 + \frac{1}{\varsigma} (w_{i,1})^2, 1\right)\right). \quad (5)$$

2.1 Gradients for $\psi_{j,t}$ and $\beta_{i,t}$

Ignoring any $y_{i,j,t} = \text{NA}$, The log posterior that we are trying to maximize is the following:

$$p(y_{i,j,t} \mid \psi_{j,t}, \zeta_{j,t}, \beta_{i,t}) \propto \sum_{i=1}^I \sum_{t=1}^T \sum_{j=1}^{J_t} \log(\text{Bern}(y_{i,j,t} \mid \theta_{i,j,t})) \quad (6)$$

Then, to derive gradients for $\psi_{j,t}, \zeta_{j,t}, \beta_{i,t}$, we compute some intermediate gradients. First, we derive gradients based on the probability a judge votes yes, i.e. $p_{i,j,t}$. The gradient is the following:

$$\frac{d}{dp_{i,j,t}} \text{Bern}(y_{i,j,t} \mid p_{i,j,t}) = \frac{y_{i,j,t}}{p_{i,j,t}} + \frac{1 - y_{i,j,t}}{1 - p_{i,j,t}}. \quad (7)$$

Next, we derive the gradient of the shifted and scaled Beta distribution:

$$\frac{d}{db_{i,j,t}} G(b_{i,j,t}) = g(b_{i,j,t}). \quad (8)$$

Finally, we take the derivative of $e(\psi_{j,t}, \zeta_{j,t}, \beta_{i,t})$ with respect to $\psi_{j,t}$ and $\zeta_{j,t}$:

$$\frac{d}{d\psi_{j,t}} e(\psi_{j,t}, \zeta_{j,t}, \beta_{i,t}) = -2(\arccos(\cos(\psi_{j,t} - \beta_{i,t})))\text{sign}(\sin(\psi_{j,t} - \beta_{i,t})), \quad (9)$$

$$\frac{d}{d\zeta_{j,t}} e(\psi_{j,t}, \zeta_{j,t}, \beta_{i,t}) = 2(\arccos(\cos(\zeta_{j,t} - \beta_{i,t})))\text{sign}(\sin(\zeta_{j,t} - \beta_{i,t})), \quad (10)$$

$$(11)$$

Here, $e(\psi_{j,t}, \zeta_{j,t}, \beta_{i,t}) = \{\arccos(\cos(\zeta_{j,t} - \beta_{i,t}))\}^2 - \{\arccos(\cos(\psi_{j,t}, \beta_{i,t}))\}^2$.

As a result, we have the following gradients for $\psi_{j,t}$ and $\zeta_{j,t}$:

$$\frac{d}{d\psi_{j,t}} p(y_{i,j,t} | \psi_{j,t}, \zeta_{j,t}, \beta_{i,t}) = \sum_{i=1}^I -2 \left(\frac{y_{i,j,t}}{\theta_{i,j,t}} + \frac{1 - y_{i,j,t}}{1 - \theta_{i,j,t}} \right) \mathbb{I}(y_{i,j,t} \in \{0, 1\}) \quad (12)$$

$$g(e(\psi_{j,t}, \zeta_{j,t}, \beta_{i,t}))(\arccos(\cos(\psi_{j,t} - \beta_{i,t})))\text{sign}(\sin(\psi_{j,t} - \beta_{i,t})), \quad (13)$$

$$\frac{d}{d\zeta_{j,t}} p(y_{i,j,t} | \psi_{j,t}, \zeta_{j,t}, \beta_{i,t}) = \sum_{i=1}^I 2 \left(\frac{y_{i,j,t}}{p_{i,j,t}} + \frac{1 - y_{i,j,t}}{1 - p_{i,j,t}} \right) \mathbb{I}(y_{i,j,t} \in \{0, 1\}) \quad (14)$$

$$g(e(\psi_{j,t}, \zeta_{j,t}, \beta_{i,t}))(\arccos(\cos(\zeta_{j,t} - \beta_{i,t})))\text{sign}(\sin(\psi_{j,t} - \beta_{i,t})). \quad (15)$$

$$(16)$$

3 Sensitivity analysis

In this Section we provide a more detailed comparison of the results under the main hyperpriors described in Section 3.2 of the main manuscript and those under the alternative prior described in Section 5.3.

Figure 2 compares the induced marginal prior on $\beta_{i,t}$ (the ideal point of justice i at time t) and $\theta_{i,j,t}$ (the probability that a justice will vote to affirm a lower court decision). The general shape of both priors is similar, but we can see that the prior on $\beta_{i,t}$ is more concentrated around 0 (which, in principle, should favor results that are closer to those obtained under a Euclidean geometry) and that the prior on $\theta_{i,j,t}$ places comparatively less mass on values of closer to either 0 or 1.

Figure 3 presents histograms of the posterior of the hyperparameters μ , ρ , τ^2 , ς and λ under both hyperpriors. As we discussed in Section 5.2 of the main manuscript, the posterior distributions seem to be robust to the prior choice. The main effect of the new priors can be seen on μ and τ^2 . For these two parameters, the alternative priors favor larger values a priori. This translates into posterior distributions that also favor slightly larger parameter values. Nonetheless, the differences are minimal. The posteriors for ρ , ς and λ appear unchanged.

Finally, Figures 4 and 5 compare the estimates of the ideal points under both sets of priors for the same 8 judges discussed in Figures 6 and 7 of the main manuscript. Note that the trajectories estimated for the five judges in Figure 4 are virtually identical under both priors. In the case of Figure 5, the trajectory of Justice William Douglas seems unchanged under the alternative prior, although the uncertainty during the mid 50s seems to go slightly down under the alternative prior. The main difference we observe in the results is in the estimates for Justices Hugo Black and Felix Frankfurter. While the general features of the trajectories of these two justices are very similar, the respective ‘‘peaks’’ that appear in 1951 under the original prior

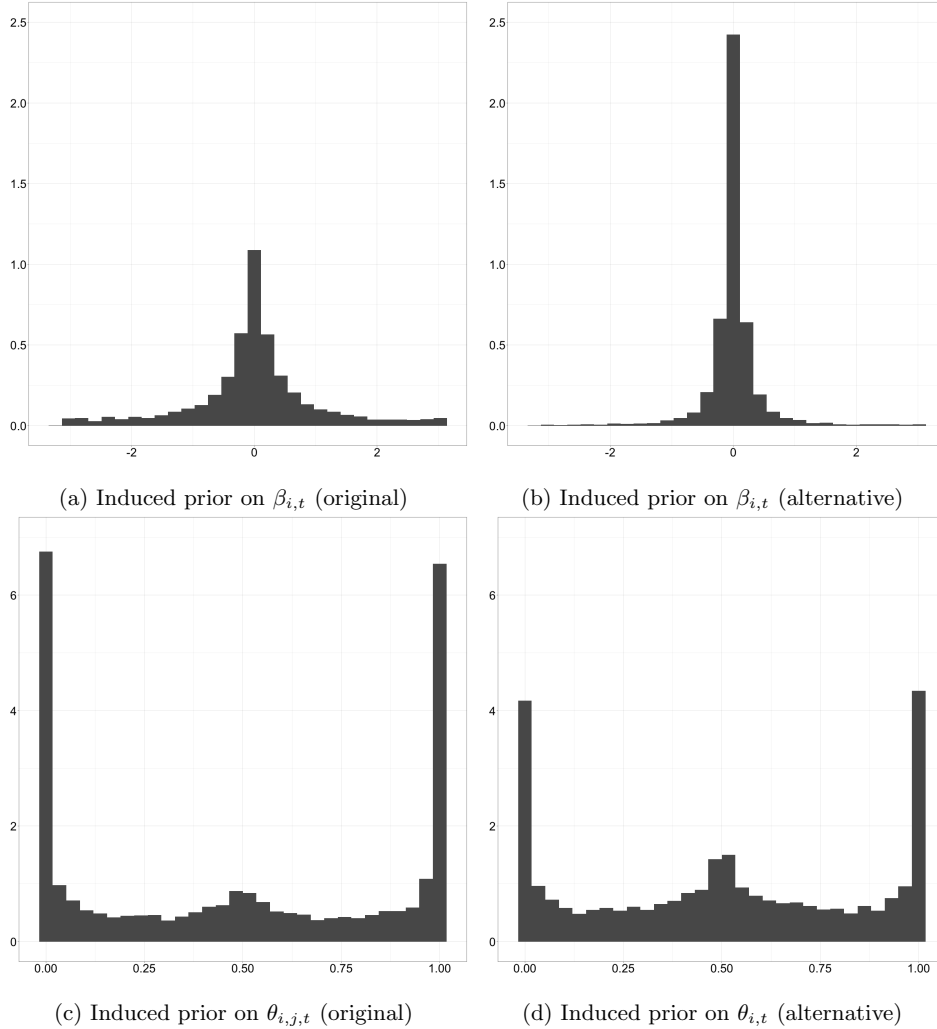


Figure 2: Histograms showing 10,000 draws from the induced marginal distribution of $\beta_{i,t}$ (top row) and $\theta_{i,j,t}$ (bottom row) under the main prior in Section 3.2 (left column) paper and the alternative alternative prior in Section 5.3 (right column).

disappear under the alternative prior. The fact that the trajectories of these justices are slightly smoother under the alternative prior is probably due to the fact that the alternative prior seems to favor slightly higher values for the autocorrelation parameter, ρ . We note, however, that this slight difference under the two priors does not change the broader picture discussed in Section 5.1 of the main manuscript.

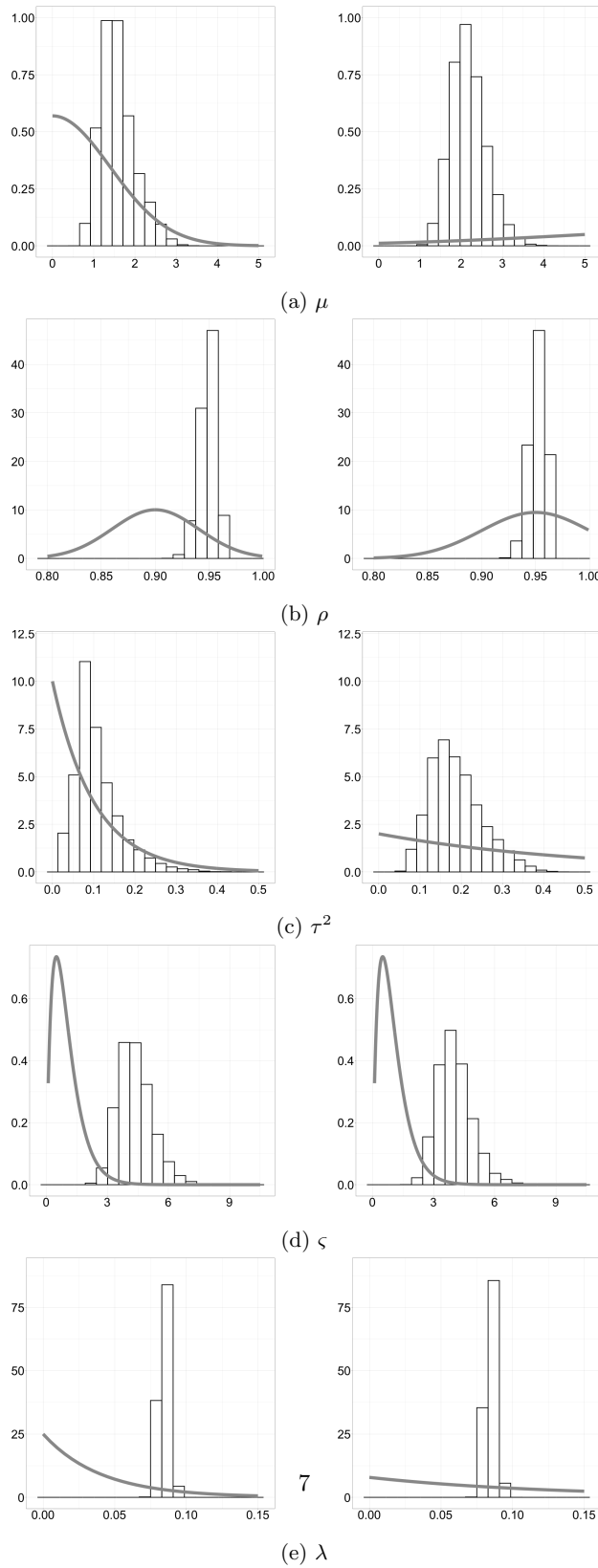


Figure 3: Histogram of the posterior distribution of various hyperparameters under the main prior (left column) and the alternative prior (right column). Solid lines correspond to the respective prior distributions.

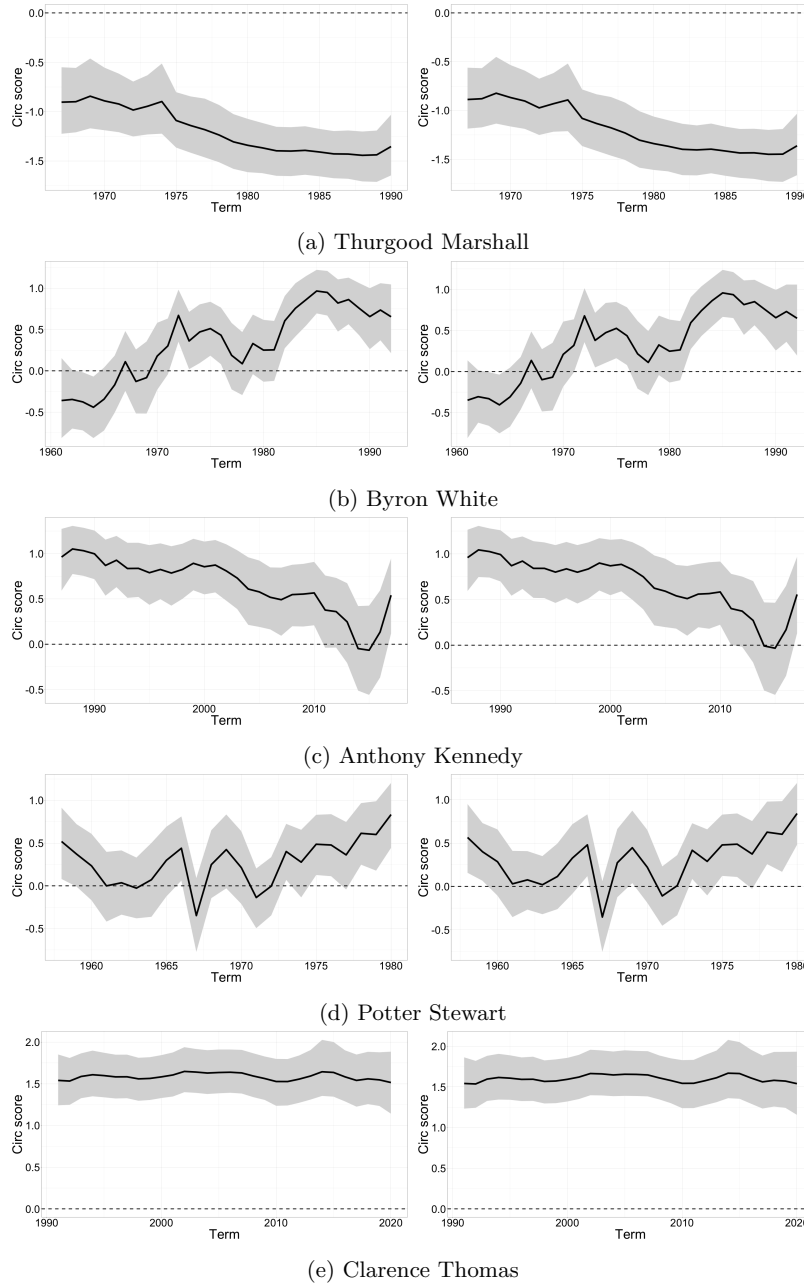


Figure 4: Posterior mean (solid line) and 95% credible intervals for the ideal points of justices Thurgood Marshall, Byron White, Anthony Kennedy, Potter Stewart, and Clarence Thomas. The left column displays estimates based on our circular model, whereas the right column displays the estimates based on the alternative prior.

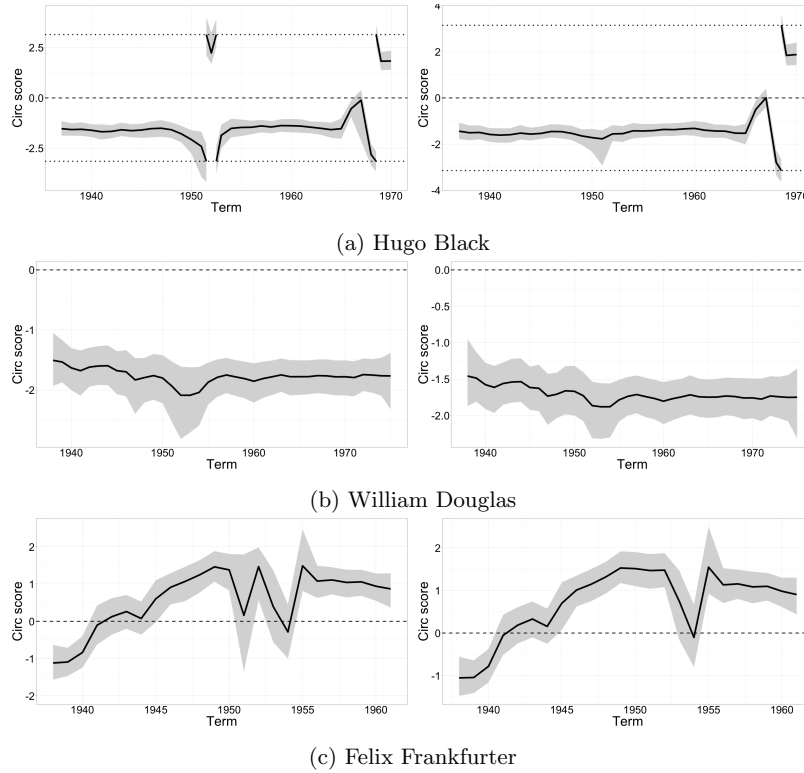


Figure 5: Posterior mean (solid line) and 95% credible intervals for the ideal points of justices William Douglas, justice Hugo Black and Felix Frankfurter. The left column displays estimates based on the prior discussed in the paper, whereas the right column displays the estimates based on the alternative prior. Zero is indicated by a dashed line and $\pm\pi$ by a dotted line.